Current Medicinal Chemistry, 2003, *10*, 2231-2252

Progress in Clinical, Pharmacological, Chemical and Structural Biological Studies of Huperzine A: A Drug of Traditional Chinese Medicine Origin for the Treatment of Alzheimer's Disease

Hualiang Jiang[1,2], Xiaomin Luo[1,2] and Donglu Bai*[2]

[1]*Drug Discovery and Design Center and* [2]*State Key Laboratory of Drug Research, Shanghai Institute of Materia Medica, Shanghai Institutes for Biological Sciences, Chinese Academy of Sciences, 555 Zu Chong Zhi Road, Zhangjiang Hi-Tech Park, Shanghai 201203, China*

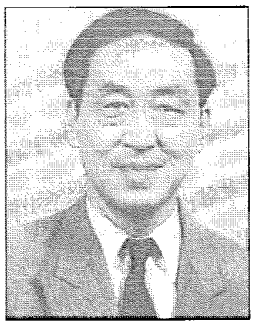

Abstract: HupA is a potent, reversible AChEI, which crosses the blood-brain barrier smoothly, and shows high specificity for AChE with a prolonged biological half-life. It has been approved as the drug for the treatment of AD in China, and marketed in USA as a dietary supplement. HupA has been the subject of investigations by an ever-increasing number of researchers since 1980's. In the last four years, HupA has been further studied in many aspects such as the chemical synthesis, structural modification, structure-activity relationship, various biological effects, and mechanisms of action. A number of papers dealing with the computational modeling and X-ray crystallographic studies of HupA-AChE complex have also been published. This review represents a comprehensive documentation of the progress in the studies on HupA during the period of 1999-2002.

Keywords: Huperzine A, Alzheimer's disease, Acetylcholinesterase, X-Ray crystallography, Molecular modeling.

1. INTRODUCTION

Alzheimer's disease (AD) is a progressive neurodegenerative disorder which affects 5% of the people over 65 years and more than 20% at ages over 80 years [1]. Nowadays AD is considered to be the third major cause of death in the developed countries after cardiovascular diseases and cancer. Although AD is a multifactorial disease, there are two major therapeutic strategies for the treatment of AD. The first strategy is to prevent the deposition of β-amyloid peptide (Aβ) as insoluble amyloid plaques, which may represent the key pathological event. Therefore, any compounds capable of diminishing or preventing the generation or deposition of Aβ could be the drug candidates to slow down the progression of the disease [2]. The second strategy is based on the cholinergic hypothesis of cognitive dysfunction [3]. This hypothesis postulates that the cognitive decline in AD patients results from a deficiency in neurotransmitter acetylcholine (ACh). In AD patient brains, the cholinergic neurons are markedly damaged together with a defect in acetylcholinesterase (AChE) and choline acetyltransferase [4]. In clinics, tacrine, donepezil and exelon are the only drugs currently used for the treatment of AD which act at the synaptic level via the inhibition of AChE [5]. These AChE inhibitors (AChEIs) cause a significant increase in ACh level in brain.

More recently, it was found that AChE tend to be deposited within amyloid plaques associated with Aβ, resulting in the formation of stable complexes causing an increase in the neurotoxicity of Aβ [6]. This is the reason why the researchers still focus their attention on the new AChEIs for the treatment of AD.

The chemistry and pharmacology of Huperzine (HupA, **1**) were first studied by the Chinese researchers in 1980's. HupA is a potent, reversible AChEI, which crosses the blood-brain barrier smoothly, and shows high specificity for AChE with a prolonged biological half-life. It has been approved as the drug for the treatment of AD in China, and marketed in USA as a dietary supplement. HupA has been the subject of investigations by an ever-increasing number of researchers since 1980's. Several review articles appeared before 2002 provided excellent coverage on chemistry, pharmacology, clinic trials and computational modeling studies of HupA [7-11]. In the last four years, HupA has been further studied in many aspects such as the chemical synthesis, structural modification, structure-activity relationship, various biological effects, and mechanisms of

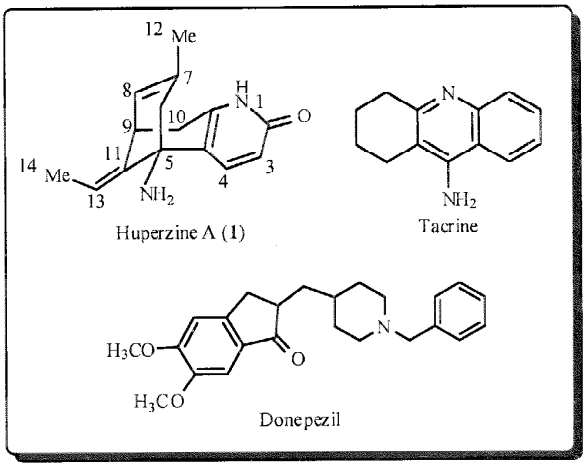

*Address correspondence to this author at the Shanghai Institute of Materia Medica, Chinese Academy of Sciences, 555 Zu Chong Zhi Road, Zhangjiang Hi-Tech Park, Shanghai 201203, China; Tel:+86-21-50806600, ext. 3520; Fax: +86-21-50807088; E-mail: dlbai@mail.shenc.ac.cn

0929-8673/03 $41.00+.00

action. A number of papers dealing with the computational modeling and X-ray diffraction studies of HupA-AChE complex have also been published. This review represents a comprehensive documentation of the progress in the studies on HupA during the period of 1999-2002.

2. CLINICAL TRAILS

A few of clinical trials were conducted in China. The results indicate that HupA is an effective and safe drug to improve the cognitive function in the aged people. Sun and co-workers [12] reported that HupA enhanced the memory and learning performance of adolescent students. With a double blind and matched-pair method, 34 pairs of junior middle school students complaining of memory inadequacy were divided into two groups. The memory quotient of the students receiving HupA was higher than those of the placebo group, and the scores on Chinese language lessons in the treated group were also elevated markedly. They also finished a test in AD patients [13]. Sixty AD patients were divided into two groups taking HupA (4°¡50 μg, p.o., bid, for 60 days) in capsules and tablets, respectively. There were significant differences on all the psychological evaluations between "before" and "after" the 60 days trials for the two groups. No severe side effects except moderate to mild nausea were observed. HupA is able to reduce the pathological changes of the oxygen free radicals in plasma and erythrocytes of AD patients as well.

Ma *et al.* [14,15] reported the double-blind trials of HupA on cognitive deterioration in 314 cases of benign senescent forgetfulness, vascular dementia and AD. The first clinical trial was conducted by the double blind method on 120 patients of age-associated memory impairment with memory quotient <100. The dosage was 0.03 mg, i.m., bid for 14-15 days. The effective rates were 68.3% and 26.4%, respectively, in two groups. No significant side effects were observed. The second trial was conducted on 88 patients of age-associated memory impairment. The dosage was 0.1 mg HupA, po, qid, for 14-15 days. The effective rates for the treated and control groups were 68.2% and 34.1%, respectively. No significant side effects were observed except for gastric discomfort, dizziness, insomnia and mild excitement.

Another trial of 25 cases with vascular dementia and 55 cases with AD were conducted with a dosage of 0.1 mg HupA, p.o., qid, for 14-15 days. The memory quotient increase of the treated group was significantly higher than that of the control. The effective rate of the treated group was 60%, significantly higher than 35% of the control. No marked side effects were observed.

3. PRETREATMENT AGAINST NERVE AGENT POISONING

In 1999, Ashani *et al.* [16] first reported that the minor toxic symptoms observed with HupA-treated monkeys following intoxication with soman; together with the results from the prophylaxis in mice, they suggested that HupA was a promising antidote and prophylactic drug against nerve agents. Later on, Lallement *et al.* [17,18] reported the efficacy of HupA in preventing soman-induced seizures, neuropathological changes and lethality in guinea pigs. HupA pretreatment at 0.5 mg/kg, i.p., totally prevented seizures and ensured the survival of all animals for 24 h after intoxication. Hippocampal tissue was then free of any neuronal damage. This efficacy seems to be related to a protection by HupA of both periferal and central stores of AChE. Organophosphonate nerve agents such as soman are potent irreversible inhibitor of central and peripheral AChEs. Pretreatment of nerve agent poisoning relies on the subchronic administration of a reversible AChEI. The protective effects against soman toxicity of pyridostigmine, physostigmine and HupA were compared in guinea pigs and monkeys. During intoxication, the cumulative dose of soman needed to produce convulsions and epileptic activity was 1.55-fold higher in the monkeys pretreated with HupA compared to those pretreated with pyridostigmine [19-22].

In summary, HupA is more stable than the carbamates used as pretreatment for organophosphonate poisoning, and the HupA-AChE complex has a longer life than other prophylactic sequestering agents. HupA has now been proposed as a pretreatment drug for nerve agent toxicity by protecting AChE from irreversible organophosphonate poisoning-induced phosphonylation. HupA was found to have antifeedant and insecticidal activities against the Australian carpet beetle, the Australian sheep blowfly and the webbing clothes moth [23].

4. PHARMACOLOGICAL ACTIONS

4.1. Effects on Learning and Memory in Animals

The effects of HupA on learning and memory have been extensively studied by Tang and co-workers [24,25]. The effects of HupA on nucleus basalis magnocellularis lesion-induced spatial working memory impairment was tested by means of a delayed-nonmatch-to-sample radial arm maze task. Unilateral nucleus basalis magnocellularis lesion by kainic acid impaired rat's ability to perform this task. This working memory impairment could be ameliorated by HupA [24]. HupA ameliorates the impaired memory naturally occurring or induced by scopolamine in aged rats. Morris water maze was used to investigate the effects of HupA on the acquisition and memory impairment of aged rats with memory impairments. During 7-day acquisition trials, aged rats took longer latency to find the plateform. HupA at dosage 0.1-0.4 mg/kg, s.c., could significantly reduce the latency or reversed the memory deficits induced by scopolamine [25].

The effects of HupA on disruption of spatial memory induced by muscarinic antagonist scopolamine and $GABA_A$ against muscimol in passive avoidance task was tested in chick. The avoidance rate was used to evaluate memory retention. Both scopolamine (100 ng) and muscimol (50 ng) injected intracranially 5 minutes before training, resulted in a decreased avoidance rate. HupA (25 ng), injected intracranially 15 minutes before training, reversed memory deficits at 30 minutes after training, and persisted at least 1 hour. The improving effects exhibited a bell-shaped dose-response curve. The results indicate that HupA improved the process of memory formation not only by acting as a highly

potent and selective AChEI but also by antagonizing effects mediated *via* the $GABA_A$ receptors [26].

Reserpine (0.1 mg/kg, i.m.) or yohimbine (0.01 mg/kg, i.m.) induces significant impairments in the monkey's ability to perform the delayed response task. HupA at dosage of 0.01 mg/kg, i.m. for the reserpine-treated monkeys and 0.01-0.1 mg/kg, i.m. for the yohimbine-treated monkeys markedly improved the memory impairments. The effects exhibited an inverted U-shaped dose-response pattern. The data suggest that HupA may improve working memory *via* an adrenergic mechanism [27].

It was reported that subchronic administration of HupA did not induce deleterious effects on spatial memory in guinea pigs [28]. A systematic comparison of tolerances between the mixed acetyl-butyryl-cholinesterase inhibitors and selective AChEIs such as HupA indicated that they showed a remarkably similar profile of behavioral symptoms associated with overdosing in rats [29].

4.2. Effects on Cerebral NMDA Receptors

Accumulating evidences suggested that effects of AChEIs on targets other than AChE in brain might also contribute to the clinical benefits in AD patients and the nootropic effects in animal models. It was found in 1997 by Ved *et al.* [30] that pretreatment of rat brain cell cultures with HupA, reduced cell toxicity and calcium mobilization both induced by glutamate. The data suggested HupA could be a potent neuroprotective agent not only where cholinergic neurons are impaired but also glutamatergic functions are compromised.

The antagonist effects of six AChEIs on *N*-methyl-D-aspartate (NMDA) receptors in rat cerebral cortex were compared by means of [^{3}H]-dizocilpine (MK-801) binding to synaptic membrane method. The rank order of potency is tacrine ≈ HupA > physostigmine > donepezil > HupB >> galanthamine. There is no correlation between their activities to inhibit [^{3}H]-MK-801 binding and AChE. The results suggested that most available AChEIs exhibited an antagonist effect on NMDA receptor in rat cerebral cortex [31]. The inhibition of two enantiomers of HupA on rat cortical AChE is highly stereospecific. However, they inhibit NMDA receptor in rat cerebral cortex without stereoselectivity [32]. The protective effect of HupA against the glutamate-induced excitotoxicity may be related to an inhibition of the NMDA receptors.

Recently, the mechanism was explored by Hu *et al.* [33,34] using whole-cell voltage-clamp recording in CA1 pyramidal neurons acutely dissociated from rat hippocampus. HupA reversibly inhibited the NMDA-induced current whereas it had no effect on the current induced by α-amino-3-hydroxy-5-methyl-4-isoxazole propionate or kainite. Changing the concentrations of L-glutamate and L-glycine did not alter the inhibitory potency of HupA, suggesting that HupA was unlikely to interact with the glutamate or glycine-binding site of NMDA receptor. In contrast, spermidine dose-dependently attenuated the inhibitory effect of HupA. Saturation binding studies revealed that HupA exerted a negative allosteric modulation on the MK-801 binding site within the NMDA receptor-channel. These results suggest that HupA acts as a non-competitive antagonist of NMDA receptor *via* interaction with one of the polyamine binding sites. The use of NMDA receptor antagonists as neuroprotective agents has become a new strategy to ameliorate the cognition deficits in AD patients.

Although HupA has been implicated to interact with cholinergic receptors, it has no effect at 100 μM on muscarinic or nicotinic receptors. HupA most likely attenuates excitatory amino acid toxicity by blocking the NMDA ion channel and subsequent Ca^{++} mobilization. HupA may protect against diverse neurodegenerative states during ischemia or AD [35].

4.3. Effects in Protection of Neuronal Cells Against β-Amyloid Induced Injury

The deposition of amyloid β-peptide (Aβ) has been suggested as the central disease causing and promoting event for the neurodegenerative diseases, and the pathological role of Aβ is partially mediated by oxidative stress. Tang *et al.* [36,37] compared the effects of HupA and tacrine on Aβ-induced cell lesion, level of lipid peroxidation and antioxidant enzyme activities in rat pheochromocytoma line PC12 cells (PC12) and primary cultured cortical neurons. Pretreatment of the cells with HupA and tacrine(0.1-10 μM) prior to Aβ 25-35 exposure significantly elevated the cell survival, glutathione peroxidase (GSH-Px) and catalase (CAT) activities, and decreased malondialdehyde (MDA) level and superoxide dismutase (SOD) activity. Either drug has similar protection against Aβ 25-35 insult.

It was found that suppressive action produced by Aβ 31-35 on long-term potentiation in rat hippocampus was NMDA receptor-independent and it was offset by HupA [38]. Tang and co-workers [39] examined the potential of HupA to antagonize the deleterious neurochemical, structural and cognitive effects induced by infusing Aβ 1-40 into the cerebral ventricles of rats. Daily intraperitoneal administration of HupA for 12 days produced prominent reversals of the Aβ-induced deficits in learning a water maze task. This treatment also reduced the loss of choline acetyltransferase activity in cerebral cortex, and the neuronal degeneration. In addition, HupA partially reversed the down-regulation of anti-apoptotic bcl-2 and the up-regulation of pro-apoptotic bax and p53 proteins, and reduced the apoptosis that normally occurred following Aβ injection. The effects of HupA on Aβ 25-35-induced neuronal apoptosis and potential mechanisms in primary cultured rat cortical neurons were also reported by Tang *et al.* [39]. Pretreatment of the cells with HupA (0.1-10 μM) prior to Aβ 25-35 exposure significantly elevated the cell survival and reduced the Aβ-induced nuclei fragmentation. HupA reduced the Aβ 25-35-induced reactive oxygen species (ROS) formation in a dose-dependent manner, and 1 μM of HupA attenuated the Aβ 25-35-induced caspase-3 activity at 6, 12, 24, and 48 h (check here!) post-treatment. The results provided the first direct evidence that HupA protects neurons against the Aβ 25-35-induced apoptosis *via* the inhibition of ROS formation and caspase-3 activity [40, 41].

(+)-HupA, the enantiomer of HupA is a less potent AChEI. The effects of (+)-HupA and (-)-HupA on the Aβ 25-35-induced injury were compared in PC12 and NG108-15 neuroblastoma cell lines. Preineubation with (+)- or (-)-

HupA (0.1-10 μM) enhanced cell survival significantly. The potency of two enantiomers in protecting cells against Aβ toxicity was similar. The neuroprotective properties of HupA enantiomers have no relation to anti-AChE activity [42].

All the results mentioned above indicate that HupA exerts the neuroprotective effects against Aβ toxicity, which may be important and may contribute to its clinical efficacy for AD treatment.

4.4. Effects in Protection on Neuronal Cells Against Free Radicals

It was found that the levels of MDA and the Mn-SOD activities in hippocampus, cerebral cortex and serum of aged male rats were 1.8-2.8 times higher than those of adult male rats. HupA (0.05 mg/kg, i.g.) lowered markedly the levels of MDA and the activities of Mn-SOD in aged male rats following 7-14 days consecutive administrations. The MDA levels in hippocampus, cerebral cortex and serum were decreased by 52.6-54.7%. The Mn-SOD activities lowered by 56.0-74.2%. The results indicated that HupA improved the abnormal free radicals in aged rats [43]. The effects of HupA on hydrogen peroxide induced cell lesion, level of lipid peroxidation and antioxidant enzyme activities were examined in rat PC12. Pretreatment of the cells with HupA (0.1-10.0 μM) prior to hydrogen peroxide exposure significantly enhanced the cell survival and antioxidant enzyme activities, and decreased the level of MDA. The results showed that HupA had protective effects against the free radical induced cell toxicity [44].

4.5. Effects in Protection of Neuronal Cells Against Hypoxia-ischemia Injury

Tang and co-workers [45] examined the beneficial effects of Hup A in the cerebral ischemia model. Permanent bilateral ligation of the common carotid arteries in rats is a chronic cerebral hypoperfusion model, which results in significant reduction of cerebral blood flow and causes learning and memory impairments and neuronal damage resembling those in AD. Daily oral administration of HupA produced a significant improvement of the deficit in the learning of the water maze task, beginning 28 days after ischemia, correlating to about 33-40% inhibition of AChE activity in cortex and hippocampus. HupA markedly restored the decrease in choline acetyltransferase activity in hippocampus, reduced the increase in SOD, lipid peroxide, lactate and glucose to their normal levels. These findings demonstrated that the improvement by HupA of the cognitive dysfunction in the late phase in chronically hypoperfused rats is due to its effects not only on the cholinergic system, but also on the oxygen free radical system and energy metabolism. They strongly suggested that HupA has therapeutic potential for the treatment of dementia caused by cholinergic dysfunction and by decrease of cerebral blood flow.

The action of HupA in cerebral ischemia in gerbils and the changes in behavior, morphology and cholinergic indices were also observed. Five minutes of global ischemia in gerbils resulted in working memory impairment. Subchronic oral administration of HupA (0.1 mg/kg, b.i.d. for 14 days) after ischemia significantly reduced the memory impairment, neuronal degeneration in the CA1 region and partially restored hippocampal acetyl transferase activity [46].

The combination of common carotid artery ligation and exposure to a hypoxic environment caused the damage in the striatum, cortex and hippocampus in the ipsilateral hemisphere, and the neuronal loss in the CA1 region of neonatal rats. HupA was administrated daily at the dose of 0.1 mg/kg, i.p. for 5 weeks after hypoxic-ischemic injury. The significant protection on behavior and neuropathology was produced. These findings suggested that HupA might be beneficial in the treatment of hypoxic-ischemic encephalopathy in neonates [47].

Serum deprivation induced apoptosis of rat primary cortical neurons, accompanying by enhanced caspase-3 activity and the release of cytochrome C into the cytosol from mitochondria. Pretreating the neurons for 2 hours with HupA (0.1-10 μM) improved neuronal survival. HupA (1 μM) significantly attenuated apoptosis by inhibiting the mitochondria-caspase pathway [48].

In support of the role for apoptosis in ischemic brain injury, several apoptosis-related genes have been found to be active in neurons. Among these genes, *c-jun, p53, bcl-2* and *bax* have been shown to play the important roles in apoptosis of different cells. It has been known that HupA, a potent AChEI also exhibited neuroprotective effects on glutamate, free radical and Aβ induced cytotoxicity [49]. Tang *et al.* [50] supposed that HupA might reduce neuronal damage during ischemia. The effects of HupA on oxygen-glucose deprivation (OGD)-induced injury were explored in rat PC12. OGD for 3 hours and reoxygenation of the cells for 24 hours triggered apoptosis. The temporal profile of *c-jun, p-53, bcl-2* and *bax* in RNA after OGD indicated that these genes played the important roles in apoptosis. Preincubation of the cells for 2 hours with 1 μM HupA significantly attenuated apoptosis. Same treatment also reduced the up-regulation of *c-jun* and *bax* as well as the down-regulation of *bcl-2*. These data suggested that the ability of HupA to attenuate apoptosis induced by OGD might result from its capability to alter the expression of the apoptosis-related genes. HupA may benefit vascular dementia and the ischemia-related neurodegenerative diseases [50].

There is a connection between oxidative stress and apoptosis, and therapeutic strategies aimed at preventing and delaying ROS-induced apoptosis might be a reasonable choice for the treatment of AD. More recently, Tang *et al* examined the effects of HupA on induction of apoptosis and the expression of the apoptosis-related genes in rat PC12 cells following exposure to hydrogen peroxide. Preincubation with HupA (1 μM) significantly prevented the cells from apoptosis, attenuated hydrogen peroxide induced over-expression of *bax* and *p53*, and rehabilitated the level of *bcl-2*. These findings suggested that HupA exerts prominent protection against the hydrogen peroxide induced apoptosis, possibly through improving expression of the apoptosis-related genes [51].

4.6. Effects on Miscellaneous Targets

It was reported that HupA inhibited nitric oxide production from rat c6 and human BT325 glioma cells [52].

The actions of HupA on the fast transient potassium current and sustained potassium current were investigated in acutely dissociated rat hippocampus neurons by Hu *et al.* [53]. HupA reversibly inhibited transient potassium current, being voltage-independent and insensitive to atropine. It also inhibited the sustained potassium current with voltage-dependency, being insensitive to atropine. In fact, the inhibition on the fast transient potassium current might form a potential toxic effect of HupA in AD treatment. In this context, HupA seems safer than tacrine, as the latter was much more potent in the inhibition of the transient potassium current. The results suggested that HupA may act as a blocker at the external mouth of the A channel [53,54].

Human studies have confirmed the analgesic action of AChEIs, such as physostigmine and neostigmine. The antinociceptive effect of HupA was also investigated in the mouse hot plate and abdominal constriction tests by Galeotti *et al.* [55]. The results showed that HupA was able to produce the dose-dependent antinociception in mice, without impairing motor coordination, by potentiating endogenous cholinergic activity. HupA is endowed by muscarinic antinociceptive properties mediated by the activation of central M_1 muscarinic receptor. So HupA and other AChEIs could be employed as analgesic for the relief of painful human conditions [55].

In conclusion, as an AChEI, HupA possesses different pharmacological actions other than hydrolysis of synaptic acetycholine. HupA has direct actions on targets other than AchE. These non-cholinergic roles of HupA could be important too in AD treatment. The therapeutic effects of HupA are probably based on a multi-target mechanism.

5. NEW SYNTHETIC APPROACHES TO HUPA AND ITS INTERMEDIATES

The multifaceted bioactivities of HupA and its scarcity in nature have provided the impetus for renewed interests in the synthesis of this target molecule. During the last four years, three groups have devoted their efforts to the syntheses of (±)-, (–)- or (+)-HupA, respectively. The Camps' group developed a route to (±)-HupA from a keto capamate **8**, which was obtained in 22% overall yield from 1,4-cyclohexanedione monoethylene ketal (Scheme 1) [56,57].

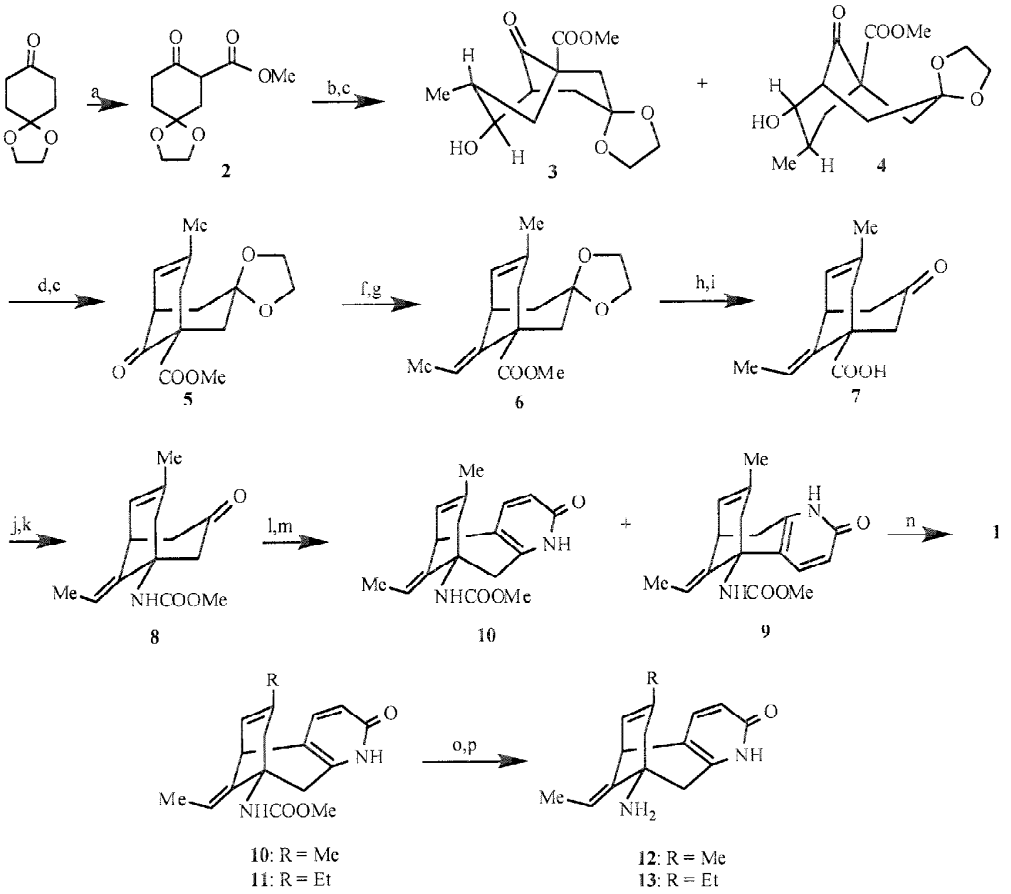

10: R = Me
11: R = Et
12: R = Me
13: R = Et

Reagents: a) Me_2CO_3, NaH/KH,THF; b) α-methylacrolein; c) TMG, CH_2Cl_2 or DBU, MeCN; d) *p*-tolyl chlorothionoformate, Py; e) pyrolysis; f) ethyltriphenylphosphonium bromide, *n*-BuLi, THF; g) thiophenol, AIBN, toluene; h) 20%NaOH,H_2O/THF/MeOH; i) 2 *N* HCl, dioxane; j) $(PhO)_2P(O)N_3$, Et_3N, chlorobenzene; k) MeOH; l) pyrrolidine, molecular sieves, benzene; m) propiolamide; n) *n*-PrSLi,HMPA; o) TMSI, $CHCl_3$; p) MeOH.

Scheme 1.

The tandem Michael–aldol reaction of **2** with α-methylacrolein gave a mixture of the bridged ring compounds **3** and **4**. Reaction of the mixture of **3** and **4** with *p*-tolyl chlorothionoformate followed by pyrolysis of the resulting thiocarbonates at 250 °C/2-4 Torr gave keto ester **5**. The hydroxy and methyl groups in both **3** and **4** are in a *trans* position; a pyrolytic *syn* elimination of the thiocarbonates was employed to achieve the dehydration to form the double bond in **5**. The Wittig reaction of **5** with ethylidenetriphenylphosphorane followed by isomerization of the mixture of (*E*)- and (*Z*)-isomers with thiophenol/AIBN afforded (*E*)-isomer **6**. Saponification of **6** with 20% aqueous NaOH in THF/MeOH under reflux followed by hydrolysis of the ketal with 2 N HCl in dioxane afforded keto acid **7**. A modified Curtis rearrangement of **7** by reaction with diphenylphosphoryl azide followed by methanolysis yielded keto carbamate **8**.

Elaboration of the pyridone ring from keto carbamate **8** was carried out by a modification of the Kozikowski group's procedures [58]. Reaction of **8** with pyrrolidine in refluxing benzene in the presence of 4 Å molecular sieves gave the corresponding enamine, which reacted with freshly prepared propiolamide in benzene under reflux furnished a mixture of regioisomeric pyridone **9** and **10**. The cleavage of the major isomer **9** with lithium 1-propanethiolate obtained HupA (1) [59]. This new approach to HupA features the elaboration of the pyridone moiety of HupA in a late stage. In this way, we can access to the different heterocyclic analogs instead of the pyridone moiety in HupA. However, the total yield of HupA was not markedly improved, compared with that of other approaches, and the purification of the isomers proved to be a tedious and difficult task.

The Langlois group [60,61] reported a formal stereoselective synthesis of (+)-HupA. The retrosynthetic analysis revealed that the skeleton of HupA could be constructed *via* an asymmetric palladium-catalyzed annulation. It was accomplished using a palladium-mediated annulation between 2-methylene-1,3-propanediol diacetate and (1*R*,2*S*)-2-phenylcyclohexanol derived β-keto ester (Scheme 2).

Transesterification of keto ester **14** with (1*R*,2*S*)-2-phenylcyclohexanol afforded the corresponding ester **15** in 84% yield. The annulation of **15** with 2-methylene-1,3-propanediol diacetate was performed with 0.1 equiv. of tetrakis(triphenylphosphine)palladium catalyst and 1.1 equiv. of 2-methylene-1,3-propanediol diacetate and TMG at room temperature for 18 hours, giving the annulated compound **16** in 75% yield.

The Wittig olefination of **16** with ethylidenetriphenylphosphorane afforded **17** as a mixture of (*Z*)- and (*E*)-isomers in 89% yield. Isomerization of the two double bonds in **17** could be conducted in a single step by treatment of **17** with triflic acid in dioxane to afford the expected compound **18** in 86% yield. The above isomerization was highly regio- and stereoselective. The resulting compound **18** was in turn quantitatively reduced with LAH in THF to give rise to the known primary alcohol **19**, a synthetic precursor of (+)-HupA. The diastereomeric excess of compound **16** is 92%.

The Terashima's group [62] first reported the palladium-catalyzed enantioselective bicycloannulation of β-keto ester **14** with 2-methylene-1,3-propanediol diacetate in 64% ee utilizing a chiral ferrocenylphosphine ligand **22**, tethering a four carbon chain with a terminal hydroxy group.

The Bai's group [63] also reported that some chiral ferroceny phosphine ligands were applied in the enantioselective bicycloannulation of **14**, and 52% ee of the product **20** was obtained (Scheme 3).

Encouraged by the above promising results, a number of new chiral ferrocenylphosphine ligands were thus prepared.

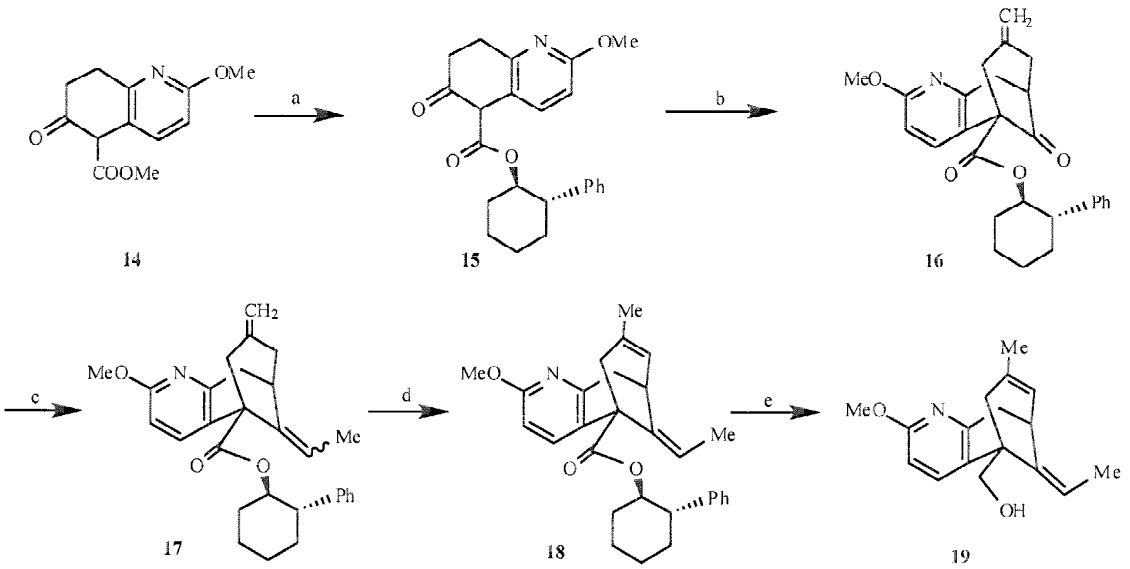

Reagents: a) (1*R*,2*S*)-2-phenylcyclohexanol, benzene,84%; b) 2-methylene-1,3-propanediol diacetate, $Pd(PPh_3)_4$, TMG, dioxane, 75%; c) $Ph_3P^+EtBr^-$, *t*-BuOK, THF, 89%; d) triflic acid, dioxane, 86%; e) LAH, THF, 100%.

Scheme 2.

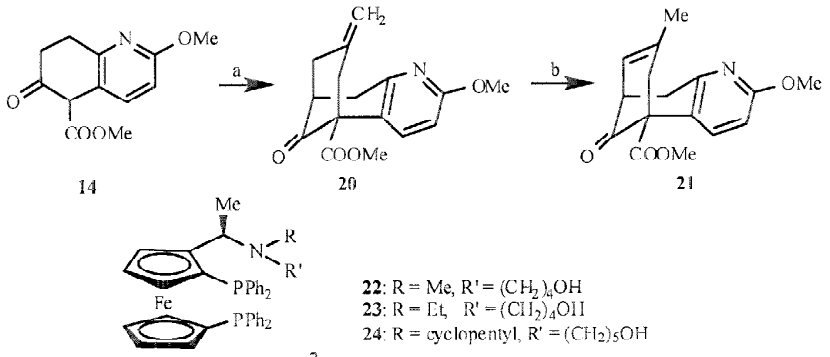

Reagents: a) 2-methylene-1,3-propanediol diacetate, (η^3-allyl)PdCl, TMG, chiral ligand, toluene; b) triflic acid, dioxane.

Scheme 3.

The enantioselectivity of the bicycloannulation in Scheme 3 was evidently improved by using ligand **23** to afford **20** in 81% ee. It was obvious that fine-tuning of the size of the *N*-substituent of the ligand with an appropriate chain length had a dramatic effect on the enantioselectivity of the reaction. Enantioselectivity of 90.3% ee for **20** was achieved using (*R,S*)-ferrocenylphosphine ligand **24** possessing a cyclopentyl group at the nitrogen. With the most efficient chiral ligand **24** in hand, the chiral non-racemic product **20** was obtained in the desired configuration for the synthesis of natural (–)-HupA. Consequently, (+)-HupA, the enantiomer of (–)-HupA, could also be obtained by using (*S,R*)-**24** as the chiral ligand [64].

Lee *et al.* [65] developed a new method for the construction of the skeleton of HupA *via* the Mn(III)-mediated oxidative radical cyclization of allylic compound **25** derived from 6-oxotetrahydroquinoline carboxylic ester **14**. The thermodynamically unstable *exo* double bond product **26** could be easily isomerized to the *endo* olefin **27** by treating it with triflic acid as reported in the literature (Scheme 4).

6. PREPARATION OF HUPA ANALOGS AND SAR STUDIES

It was reported that heptylene-linked bis-tacrine was 150-fold more potent and 250-fold more selective for AChE inhibition than tacrine, as a consequence of dual-site binding to the catalytic and peripheral active sites of AChE. The hybrid analogs **28** comprised of tacrine and HupA-like moiety were thus prepared (Table 1). The hybrids **28a-h** were all more potent AChEIs than tacrine and HupA. The most active hybrid inhibitor **28g** is 13-fold more potent than HupA [66]. It was proposed that **28g** delivered its potency and selectivity from simultaneous binding to the catalytic and peripheral sites of AChE.

Table 1. AChE Inhibition by Hybrids 28a-h[a]

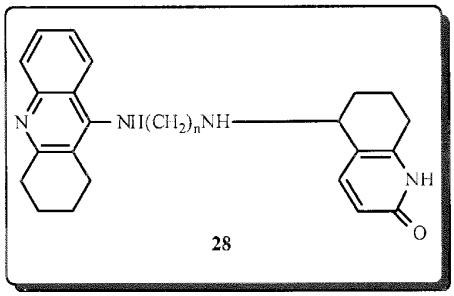

Comp.	n	AchE, IC_{50} (nM)	BChE, IC_{50} (nM)	Selectivity
28a	4	42.6	228	5.4
28b	5	122	220	1.8
28c	6	37.1	223	6.0
28d	7	53.1	233	4.4
28e	8	26.2	166	6.3
28f	9	36.3	150	4.1
28g	10	8.8	81.5	9.3
28h	12	112	434	3.9
HupA		114	135,000	1170
tacrine		223	92	0.4

[a]AChE: rat cortex homogenate; BChE: rat serum.

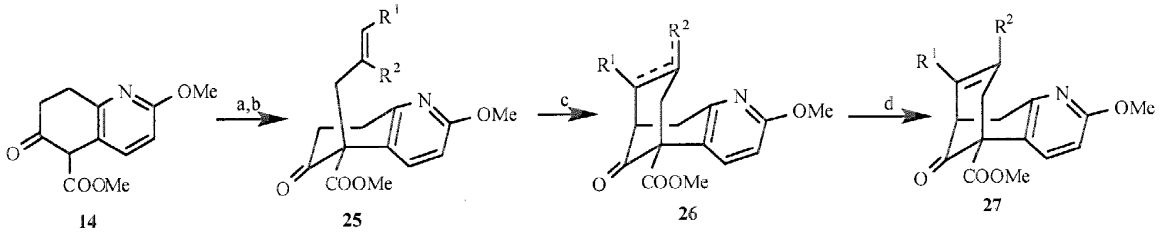

Reagents: a) NaH/DMF; b) allylic bromides; c) $Mn(OAc)_3$, $Cu(OAc)_2$, AcOH; d) triflic acid.

Scheme 4.

Table 2. AChE Inhibition by HupA Fragment Dimers[a]

compound	n	AChE, IC_{50} (nM)	BChE, IC_{50} (nM)	selectivity
(*rac,meso*)-**30h**	12	159	24400	153
(*rac,meso*)-**31h**	12	3620	60000	16.6
(*rac,meso*)-**32h**	12	5000	78900	15.8
(*S,S*)-30f	10	151	1820	12.1
(*S,S*)-30g	11	84	1160	13.8
(*S,S*)-30h	12	52	9600	185
(*S,S*)-30i	13	52	16700	321
(*S,S*)-30j	14	240	59500	248
(*R,R*)-30h	12	3130	297000	94.9
(–)-HupA		115	135000	1200
tacrine		231	77	0.3

[a]AChE: rat cortex homogenate; BChE: rat serum.

Based on the bivalency or dimer strategy, Carlier *et al.* [67] designed and prepared a number of alkylene-linked dimers of 5-amino-5,6,7,8-tetrahydroquinolin-2-one, bis(*n*)-hupyridones **30**, **31** and **32** (Table 2, *n* stands for the number of carbon of the alkylene link).

Compounds **30a-f,h** and **31c-f,h** were obtained by condensation of α,ω-diamines with keton **29a** or **29b** followed by reduction with $NaBH_4$, respectively (Scheme 5). They are mixtures of *rac*- and *meso*-diastereomers. (*rac,meso*)-Compounds **30a-f,h** showed dramatically enhanced anti AChE potency, with the highest potency observed for **30h** bearing a tether length of 12 methylene groups. Compounds **31c-f,h** were also optimized at $n = 12$, but they were less potent than **30h** (Table 2). 2-Methoxypyridine analog of **30h**, compound **32h** was prepared from **29a** (Scheme 6). It was 31-fold less potent than **30h**, suggesting that pyridone moiety contributes to binding affinity in the active site of AChE. Pure enantiomers of **30f-j** were synthesized from (*S*)- or (*R*)-**33**, respectively. Reaction of (*S*)-**33** with the corresponding α,ω-diacyl chloride, reduction of the resulting diamides with BH_3·THF followed by hydrogenolysis of the benzyl group afforded compounds (*S,S*)-**30f-j**. Accordingly, (*R,R*)-**30h** was obtained from (*R*)-**33**. Compound (*S,S*)-**30h** exhibited 60-fold greater potency than its enantiomer (*R,R*)-**30h**. The optimum leads (*S,S*)-**30h,i** possess a tether chain of 12-13 methylene groups, and are twice as potent as (-)-HupA in inhibition of AchE. Although (*S,S*)-**30h,i** are less potent than 10-*axial*-methyhuperzine [7] and the tacrine-HupA hybrids [68], they are easily prepared. Carlier *et al.* [67] demonstrated that dimerization of a simplified and inactive fragment of HupA could produce a lead with greater potency than HupA itself in inhibition of AChE.

Based on the hypothesis of two binding sites in the active gorge of AChE and the good example of bis-tacrine, a series of bis-HupA (**34**) with various lengths of the alkylene tethers were synthesized *via* reductive amination of **1** and α,ω-dialdehydes (Scheme 7) [69]. It was found that these dimers were less potent than HupA. Among them the heptamethylene dimer **34** ($n = 7$) was the must potent one, being 5-fold less potent than HupA [70].

Zeng *et al.* [71,72] reported a structural hybrid of HupA and donepezil, compound **35**, which was a mixture of four

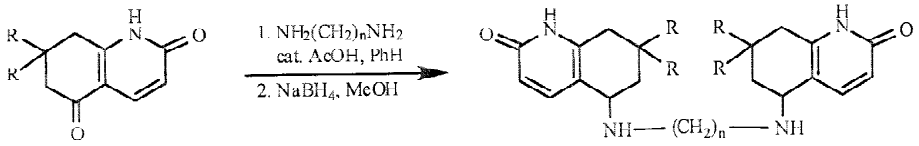

29a: R = H
29b: R = Me

rac,meso-**30a-f,h**: R = H
rac,meso-**31c-f**: R = Me

Scheme 5.

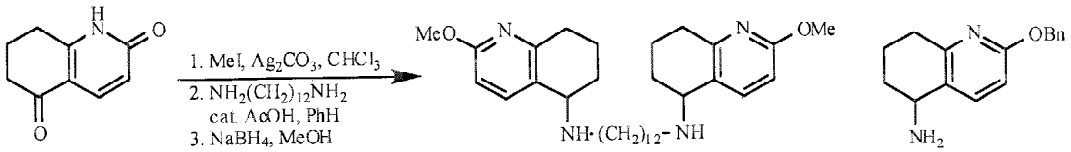

29a **32h** **33**

Scheme 6.

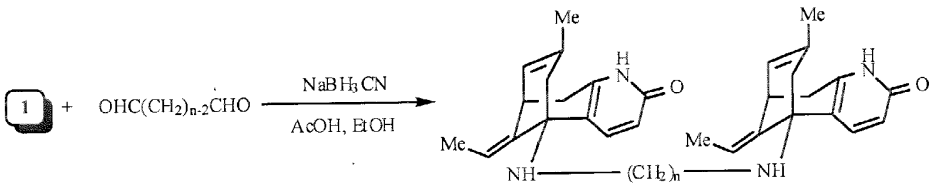

34: n = 7-12

Scheme 7.

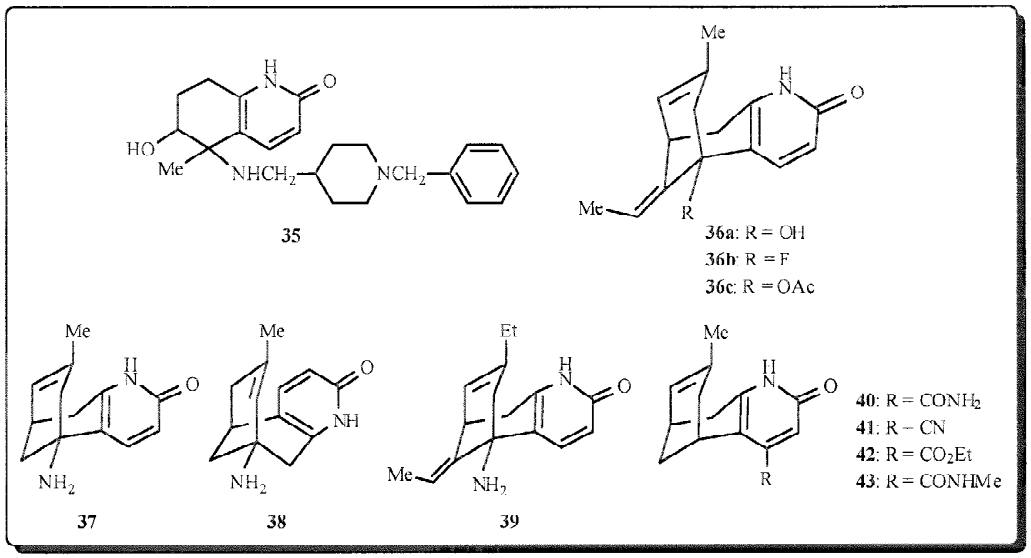

stereoisomers. The IC_{50} value of **35** was >190 μM, much higher than that of HupA (0.082 μM).

Three amino-isosteres of HupA, **36a-c** were synthesized by Zhu *et al.* [73], and their inhibitory activities against AChE were much lower than HupA. These findings suggested that the C-5 amino group in HupA plays an important role for AChE inhibitory activity.

In order to ascertain the relevance of the ethylidene substituent at C-11 in HupA to the AChE inhibitory activity, Camps *et al.* [74] prepared an 11-unsubstituted analog **37** and its regioisomer **38**. The 11-unsubstitued HupA **37** was 122-fold less potent than HupA in inhibition of AChE, the regioisomer **38** was about 1300-fold less potent.

Table 3. AChE Inhibition of 7-Ethyl-11-unsubstituted Analogs and Other Regioisomers of HupA[a]

Compound	IC_{50} (μM)
(-)-HupA	0.074
37	9.05
38	>100
39	0.870
12	25.1
13	97.1

[a]AChE from bovine erythrocytes

In the studies of a novel approach to HupA, the Camps group [59] also accomplished the preparation of 7-ethyl derivative **39** and two regioisomeric analogs, **12** and **13** of HupA through the same synthetic sequences by using α-ethylacrolein (Scheme 1). From the minor regioisomers **10** and **11**, two regioisomeric analogs of HupA were obtained. The IC_{50} values for AChE inhibition by these compounds are listed in Table **3**. Only 7-ethyl analog **39** showed a significant activity, about 12-fold less potent than (–)-HupA.

In conclusion, removal of the ethylidene group in HupA led to a pronounced decrease of the inhibitory activity, showing that this olefinic appendage is essential for high AChE inhibitory activity while replacement of the 7-methyl in HupA by an ethyl group induced a small but negative effect on the activity.

The polar group at C-4 position of HupA could mimic the interactions of C-5 amino group of HupA with the active site of AChE, Camps *et al.* [75] reported the preparation of compounds **40-43**, the 4-substituted analogs of desamino-desethylidine HupA, but no biological data for these compounds.

A convergent approach to the desamino skeleton of HupA was reported (Scheme 8) [76]. An aldol reaction between cyclohexenone and 3-bromo-1-formyl-6-methoxypyridine followed by protection of the resultant alcohol, yielding compound **44**. Intramolecular Heck reaction of **44** in the presence of Pd(0) afforded **45**, which could be used as the precursor of desamino analogs of HupA. The over yield of **45** was very low.

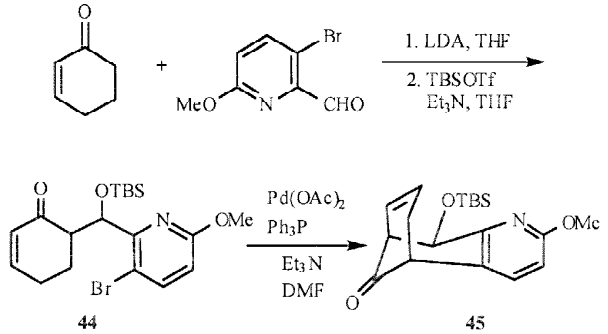

Scheme 8.

In 1996, the Kozikowski group [77] reported that the kinetic and inhibition parameters of 10,10-dimethyl HupA **46** were comparable to those of (±)-HupA in the inhibitory activity. Recently, the enantiomers of **46** were separated by HPLC over a chiral stationary phase. The (–)-enantiomer

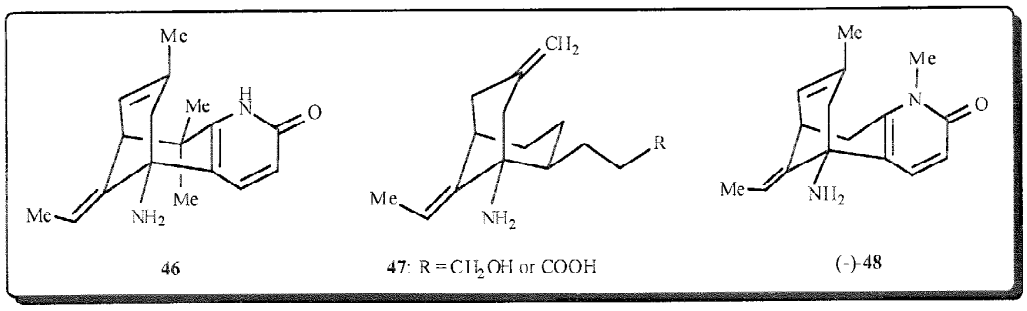

inhibited AChE with a K_i value approaching that of (–)-HupA, whereas (+)-**46** showed no activity. However, both (–)- and (+)-**46** were equally potent against the glutamate-induced neurotoxicity when tested in neurons [78].

Two HupA–like analogs **47** without the pyridone moiety were prepared [79]. (*5R,9R*)-(–)-1-Methyl HupA (**48**) was synthesized by the Bai's group [80], but its inhibitory activity of AChE was 100-fold less potent than that of (-)-HupA. Probably, the *N*-methyl group in (–)-**48** may block the formation of the hydrogen bond between the pyridone nitrogen and the protein residues in the active site of AChE.

Mulzer *et al.* [81, 82] reported the synthesis of desamino HupA **49** and its (*E*)-isomer **50** (Scheme 9). The key steps are: (1) a double Michael addition of dimethyl 1,3-acetone dicarboxylate onto benzoquinone monoketal to give **51**; (2) a regio-controlled-double bond isomerization with Pd/C–H_2 to form **52**; (3) a novel pyridine synthesis *via* the Michael addition of β-keto ester onto acrylonitrile to afford **53**; and (4) the separation of (*E*)- and (*Z*)-isomers by HPLC *via* the corresponding acetate derivatives **54**. The biological results revealed that (*E*)-isomer **49** showed about 100-fold less potent than HupA in AChE inhibition, and (*Z*)-isomer **50** is 6-fold less active than **49** (Table 4).

Table 4. Rat Brain AChE Inhibition by Desamino Analogs of HupA

Compound	K_i (μM)
(-)-HupA	0.024 – 0.040
49	2.00
50	12.3

Most recently, three hybrid analogs of HupA (**1**) and HupB (**55**) were synthesized by the Kozikowski group [83]. Hybrid analog **56** was obtained from **20** *via* a sequence of reactions as shown in Scheme 10. β-Keto ester **20** was converted into **59** by reduction and benzylation followed by hydrolysis with LiI and NaCN in DMF at reflux. Carboxylic acid **59** was subjected to the Curtius rearrangement, and the resulting isocyanate was reacted with 8 *N* HCl at 100°C to afford amino alcohol **60** with concomitant debenzylation and double bond shifting from the *exo* to the *endo* position. Michael addition of **60** with methyl vinyl ketone and oxidation of the hydroxy group with PDC provided diketone **61**. Intramolecular reductive coupling of diketone **61** using

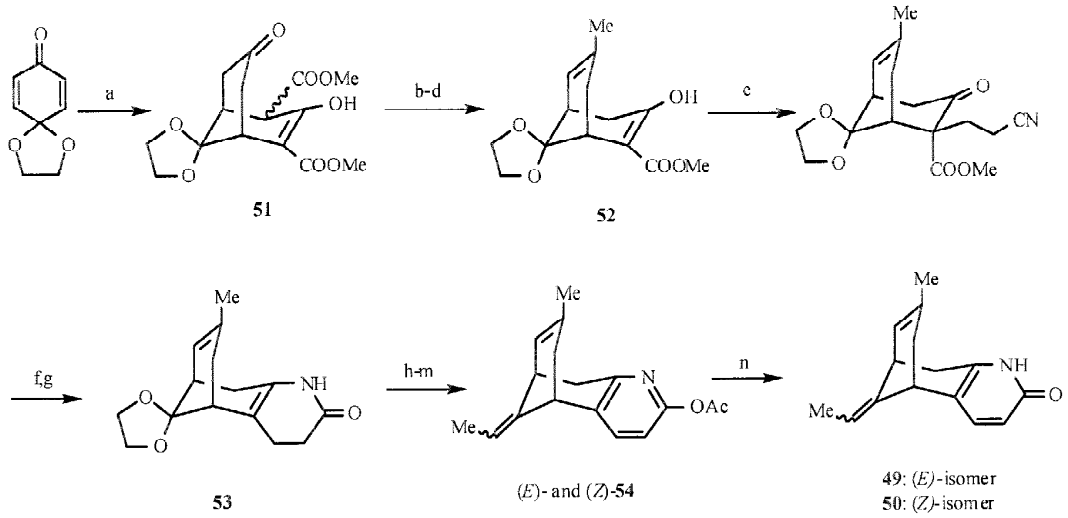

Reagents: a) $(MeO_2CCH_2)_2CO$, cat. EtONa, EtOH; b) LiOH, DMF, H_2O, 150 °C; c) $Ph_3P^+CH_3Br^-$, *n*-BuLi, THF; d) Pd/C, H_2, EtOH; e) acrylonitrile, DBU, DMF; f) LiBr, DMF, 150 °C; g)NH_3-MeOH, 120 °C, sealed tube; h) SO_2Cl_2, CH_2Cl_2 then 120 °C; i) H_2SO_4, acetone; j) $Ph_3P^+EtBr^-$, *n*-BuLi, THF; k) PhSH, AIBN, PhMe; l) Et_3N, Ac_2O, CH_2Cl_2; m) HPLC separation; n) NH_3-MeOH, CH_2Cl_2.

Scheme 9.

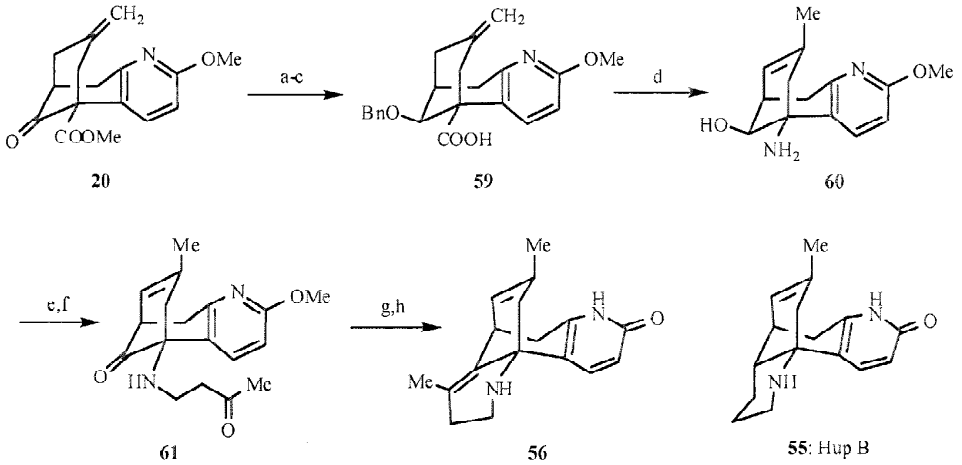

Reagents: a) $NaBH_4$, MeOH; b) BnBr, NaI, DMF; c) LiI, NaCN, DMF; d) $(PhO_2)P(O)N_3$, Et_3N, MeOH; then 8 *N* HCl; e) CH_2=ClCOMe, Et_3N, CH_2Cl_2; f) PDC, CH_2Cl_2; g) $TiCl_4$, Zn, Py, THF; h) Me_3SiI, $CHCl_3$, then MeOH.

Scheme 10.

$TiCl_4$, Zn and pyridine, and deprotection gave the final product **56**.

The hybrid analogs **57** and **58** were synthesized from amino alcohol **60** according to Scheme 11. The key intermediate **60** was acylated with the corresponding carboxylic acids, respectively, followed by oxidation with *n*-Pr_4NRuO_4/NMO providing amides **62** and **63**. Removal of the TBS group in **62** and oxidation once again of the newly formed hydroxy group gave diketone, which was treated with silica gel yielding the intramolecular aldol product **64**. Aldol condensation of ketone **63** preceded only in the presence of K_2CO_3 in EtOH to give the cylic compound, which was further reduced with DIBAL-H, affording aldehyde **65**. The thioketal of **64** was treated with Rany-Ni to give lactam **66**, which was treated with the Lawesson's reagent to afford the thiolactam. The latter was successively reduced with Rany-Ni and $NaBH_3CN$ followed by deprotection of the methoxy group led to analog **57**. In a similar fashion, aldehyde **65** was converted into analog **58** [84].

The AChE inhibitory data of the hybrid analogs **56**, **57** and **58** are listed in Table 5. Analog **56** is structurally more closely related to both HupA and HupB, but it is less active than HupA and HupB. Although **57** and **58** are racemates, they are 2- and 3.5-fold more potent than (–)-HupB, respectively. In comparison with (±)-HupA, the hybrid analogs **56**, **57** and **58** are about 10-100 times less active in AChE inhibition.

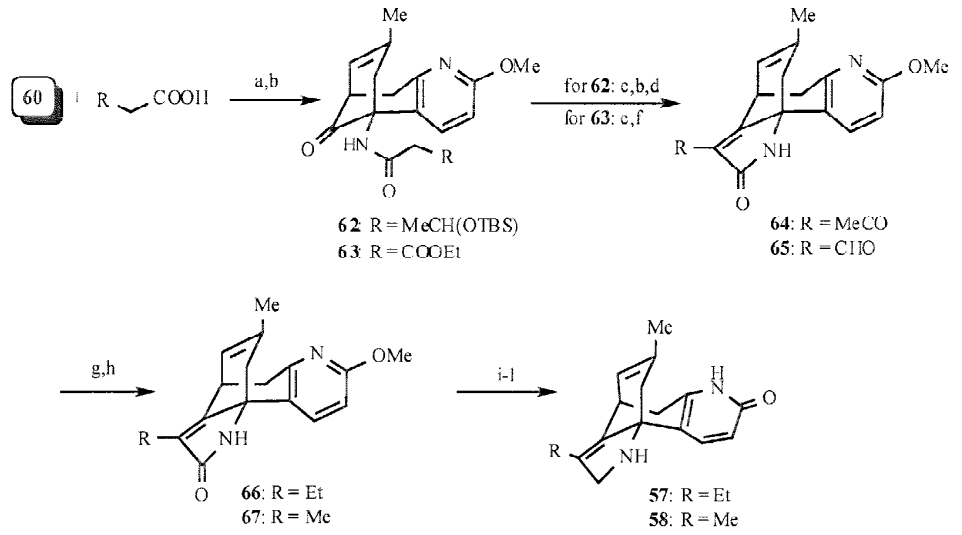

Reagents: a) DCC, HOBt, CH_2Cl_2; b) *n*-Pr_4NRuO_4, NMO, CH_2Cl_2; c) TBAF, THF; d) SiO_2; e) cat. K_2CO_3, EtOH; f) DIBAL-H, CH_2Cl_2; g) $HS(CH_2)_2SH$, $BF_3{\cdot}Et_2O$, CH_2Cl_2; h) Rany-Ni, EtOH; i) Lawesson's reagent, CH_2Cl_2; j) Rany-Ni, THF; k) $NaBH_3CN$, THF; l) Me_3SiI, $CHCl_3$, then MeOH.

Scheme 11.

Table 5. Inhibition of AChE[a] by Hybrid Analogs

Compound	K_i (μM)
(-)-HupB	0.794
(±)-HupA	0.024
56	2.05
57	0.40
58	0.22

[a]From fetal bovine serum.

Based on the structure hybridization method in medicinal chemistry, the Camps' group [85] has been involved in chemical and pharmacological studies of huprines. Huprines are the tacrine-HupA hybrids combined the 4-aminoquinoline moiety of tacrine with the bridged carbobicyclic moiety of HupA. More than 30 various huprines in racemic and optically pure forms were synthesized, and pharmacological studies of these compounds demonstrated that they are a novel class of very potent and selective AChEIs. Several huprine are more active than other known AChEIs. The first huprine to be synthesized is compound **69**, lacking the ethylidene appendage of HupA. The Friedländer condensation of enone **68** with 2-aminobenzonitrile in the presence of $AlCl_3$ in dichloroethane led efficiently to huprine **69** (Scheme 12) [85]. This compound is 2-fold more potent than tacrine hydrochloride and slightly more potent than HupA as AChEI. Huprines **70-72** are 21-, 104- and 32-fold less potent than **69**, respectively.

New huprines were designed by chemical modification of the lead structure **69** in three aspects, the C-13 methylene bridge, the unsaturated bridge between C-7 and C-11, and the benzene ring. The huprine bearing an ethylidene group at C-13, compound **74** was prepared from keto acid 7. The Barton's decarboxylation of 7 afforded enone 73 followed by the Friedländer condensation with 2-amino-benzonitrile under the routine conditions, yielding huprine **74** (Scheme 13) [85]. The (*E*)-isomer **74**, bearing an ethylidene group with the same configuration of HupA, is almost 5-fold lower than the lead compound **69** but 3.6-fold more potent than (*Z*)-isomer **75** in inhibition of AChE.

Huprine **76** exhibited an AChEI activity 32-fold lower than the lead **69**. From the pharmacological data of these huprines, it seems that for an optimal activity the C13 methylene group should be kept intact [85]. The 9-ethyl-substituted huprine 77 and 9-unsubstituted huprine **78** were found to be 1.7-fold more active and 75-fold less active as AChEI than **69**, respectively, suggesting the importance of an alkyl group at C-9 for AChEI activity [85].

Other huprines with a saturated three–carbon bridge were also prepared. Saturation of the unsaturated bridge and removal of the C-9 methyl group led to a dramatic decrease in the AChE inhibitory activity. Compound **79** is 643-fold

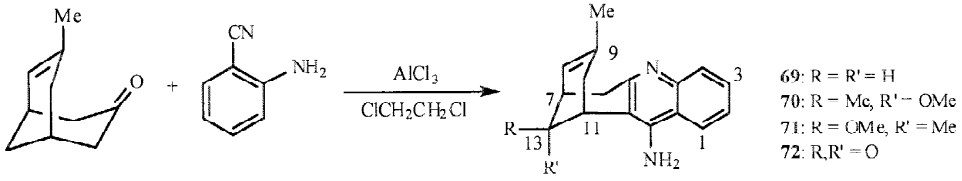

69: R = R' = H
70: R = Me, R' = OMe
71: R = OMe, R' = Me
72: R,R' = O

Scheme 12.

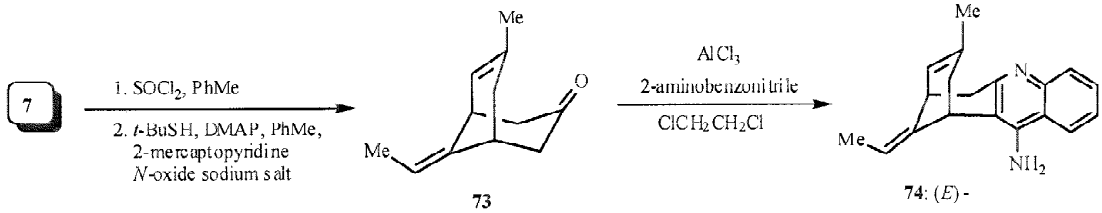

73

74: (*E*)-
75: (*Z*)-

Scheme 13.

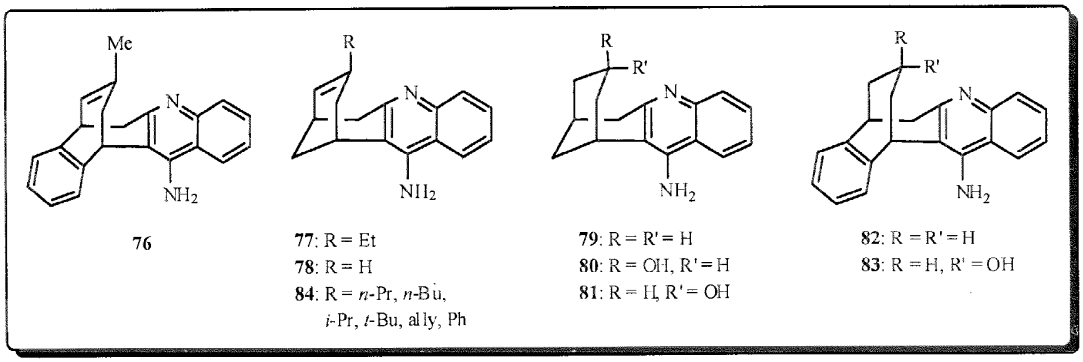

76

77: R = Et
78: R = H
84: R = *n*-Pr, *n*-Bu, *i*-Pr, *t*-Bu, ally, Ph

79: R = R' = H
80: R = OH, R' = H
81: R = H, R' = OH

82: R = R' = H
83: R = H, R' = OH

less active, **80** and **81** are 25- and 66-fold less active, and **82** and **83** are 40- and 234-fold less active than the lead compound **69**, respectively [85].

The SAR studies of huprines as mentioned above revealed that the C-13 methylene and the unsaturated bridge in **69** are the essential structural features for a good AChE inhibition. The structural variations of the lead compound **69** that lead to an improved bioactivity is the substitution of the C-9 methyl group by an ethyl group. New huprines were thus designed and prepared by the Camps group *via* substitution at C-9 with more lipophilic alkyl groups, and introduction of halogen atoms or methyl group on the benzene ring. All compounds **84**, bearing a *n*-propyl, *n*-butyl, isopropyl, *tert*-butyl, allyl or phenyl group at C-9 were found to be less active than **69** [86].

Fifteen new huprines with C-9 methyl or ethyl groups and halogen atoms or methyl group at the positions 1 and 3 or position 2 of the benzene ring were synthesized by the same methodology used for the synthesis of the lead compound **16**, using an appropriately substituted aminobenzonitrile. All of the compounds prepared are 1.6-30 fold more active in inhibiting bovine AChE than HupA, and 1.4-27 fold more active than the lead compound **69** except for the compound substituted at the position 2 with a chlorine atom [86-88].

In general, the inhibitory activity of these compounds towards human AChE is 1.1-2.0-fold more active than bovine AChE. In the case of 3-chloro-substituted huprines **85** and **86**, which are 5.4- and 3.7-fold more active towards human AChE than bovine AChE, respectively. These new huprines displayed a high selectivity in inhibiting human AChE than human BChE. 3-Chloro-substituted huprines **85** and **86** are the most potent and selective human AChEIs among them. The pharmacological data of these huprines suggest that huprines and HupA do not have the same binding mode with AChE.

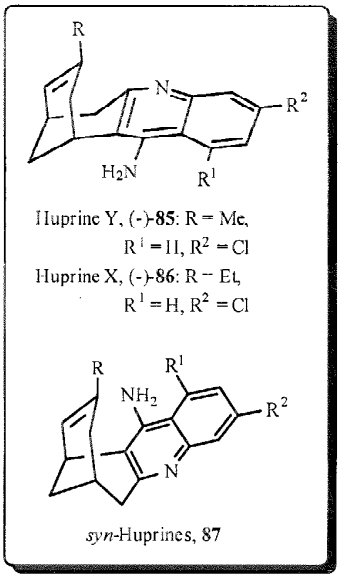

Huprine Y, (-)-**85**: R = Me, R^1 = H, R^2 = Cl

Huprine X, (-)-**86**: R = Et, R^1 = H, R^2 = Cl

syn-Huprines, **87**

Two enantiomers of **77** were obtained by stereoselective synthesis, and the racemic huprines **69**, **77**, **85**, **86** *etc.* were also successfully separated into their enantiomers, respectively, by means of medium pressure liquid chromatography using a chiral column [89,90]. In all cases, the (–)-enantiomers are the more active ones than (+)-enantiomer. Huprines (–)-**85** and (–)-**86** showed high inhibitory activity toward human AChE with IC_{50} of 0.318 and 0.323 nM, respectively. The so-called huprine Y [(–)-**85**] and huprine X [(–)-**86**] are the most promising candidates among huprines for AD treatment. Additional studies on huprines Y and X have shown that both compounds act as the tight-binding and reversible AchEIs. They cross the blood brain barrier, and bind to the human AChE with a K_i value of around 30 μM, one of the highest affinities reported in the literature. The affinity of both compounds for human AChE is 180-fold higher than that of HupA [87,88].

Solsona *et al.* [91] reported that (±)-huprine Y and X increased the level of ACh in the synaptic cleft more effectively than tacrine. The interaction of (±)-huprine X with nicotinic receptors was weaker than (±)-huprine Y, suggesting that (±)-huprine X would be more specific for maintaining the extracellular ACh concentration.

Camps *et al.* [90] reported that under the usual acidic Friedländer reaction conditions to prepare the above-mentioned huprines, *syn*-huprines **87** were also formed but rearranged *in situ* to the more stable *anti*-regioisomers, huprines. *syn*-Huprines **87** were found to be slightly less active than the corresponding *anti*-derivatives, huprines in AChE inhibition [92].

In conclusion, huprines act truly as the tacrine-HupA hybrids. The 4-aminoquinoline moiety of (–)-huprines occupies the same position in the active site of AChE as the corresponding moiety in tacrine, thus sharing all the features that modulate the binding of tacrine to AChE. Meantime, the unsaturated bridge of huprines occupies roughly the same position of the corresponding moiety in HupA, while the C-13 methylene bridge and their heterocyclic rings of (-)-huprines and HupA are positioned in opposite directions. A comprehensive review article covering the synthesis, chemical modification, and SAR exploration of this new structural family of AChI has been published in 2001 [11]. For further details, please refer to reference 11 and references cited therein.

7. X-RAY CRYSTALLOGRAPHY AND MOLECULAR MODELING STUDIES ON HUPA ANALOGS INTERACTING WITH ACHE

7.1. Structure-Based HupA Analogs Design

In the above section, we reviewed the chemistry and SAR of HupA analogs. Before discussing the interactions between HupA analogs and AChE, we summarize the design processes of some important HupA analogs based on the X-ray crystal structures of AChE or its complexes with inhibitors. Since Sussman *et al.* [93] reported the X-ray crystal structure of *Torpedo californica* AChE (*Tc*AChE), more than 30 structures of the ligand–AChE complexes have been determined by X-ray crystallography (http://www.rcsb.org/pdb/index.html). Great efforts for designing potent novel inhibitors have been undertaken based on the available three-dimensional (3D) structures of the inhibitor–AChE complexes [66,67,85-92,94,95]. The

structure-based HupA analogs design is much active during the past four years [66,67,85-92].

The X-ray crystal structures of tacrine-*Tc*AChE [96] and HupA-*Tc*AChE [97] complexes indicate that the binding sites for tacrine and (–)-HupA within *Tc*AChE are adjacent and partially overlapped [98]. Camps *et al.* [85-92] designed a series of new AChEIs, named huprines **77-87**, combining the pharmacophores of (–)-HupA and tacrine. The synthesis and bioassay of these hybrids have been reviewed in the above section. Indeed, certain hybrids, which contain the 4-aminoquinoline substructure of tacrine and the carbobicyclic moiety of HupA, but lack its ethylidene substituent, display more potent anticholinesterase activity than either tacrine or (–)-HupA [87]. Of the series, huprine X **86** showed the highest potency, which inhibited human AChE (hAChE) with an inhibition constant, K_i, of 26 pM, being about 180-fold more potent than (–)-HupA and 1200-fold more potent than tacrine [87].

The complexes of *Tc*AChE with such bisquaternary ligands as decamethonium [DECA, $Me_3N^+(CH_2)_{10}NMe_3^+$] [96] and BW284C51 [99] led to the assignment of Trp279 as the major element of a second, remote binding site, which is near the top of the active-site gorge, named the peripheral "anionic" site, ca. 14 Å apart from the active-site. These structural assignments promoted the development of bivalent AChE inhibitors **28-35**, capable of binding with the two binding sites simultaneously, to improve drug potency and selectivity [66,67,94,95]. The first example of bivalent inhibitors is the heptylene-linked tacrine dimer, bis(7)-tacrine, designed and synthesized by Pang *et al.* on the basis of computational studies [94]. Bis(7)-tacrine showed significantly higher potency and selectivity for inhibition of rat AChE than monomeric tacrine [94,95]. Later on, Carlier *et al.* [66] designed and synthesized the bivalent inhibitors **28** composed of a key fragment of HupA and an intact tacrine unit. The most active compound in this series is 13-fold more potent than HupA and 25-fold more potent than tacrine, however, their selectivity is lower than HupA (Table **1**). Recently, Carlier *et al.* [67] designed and synthesized a series of dimers **30** of hupyridone, an easily synthesized but pharmacologically inactive fragment of (–)-HupA on the basis of docking modeling. Although these HupA-like dimers are not as potent as bis(7)-tacrine or the tacrine/huperzine fragment heterodimer on rat AChE, being only 2-fold more potent than (–)-HupA for the most active compound, they are superior to the latter dimers in terms of selectivity for AChE (Table 2) [100].

7.2. Interactions between HupA Analogs and AChE Revealed by X-ray Crystal Structures

The multifold pharmacological action of HupA suggested that it might be a unique and important drug for the treatment of AD patients [24-55]. Great efforts for gaining insight into the binding feature between HupA and AChE have been devoted since 1991 when the 3D structure of the native *Tc*AChE was published by using both X-ray crystallography and molecular modeling. However, the X-ray crystal structure of (–)-HupA–*Tc*AChE was not obtained until 1997 [97]. Therefore, molecular modeling played a major role in mapping the interaction model for HupA with AChE. Considering the pharmacophoric groups, Kozikowski *et al.* [101] suggested a possible orientation for HupA parallel to the ACh molecule inside the active site of AChE. Nevertheless the X-ray crystal structure [97] indicates that the observed orientation of HupA within the active-site gorge appears to be orthogonal to the modeling result. Several other docking simulations made the similar mistake of

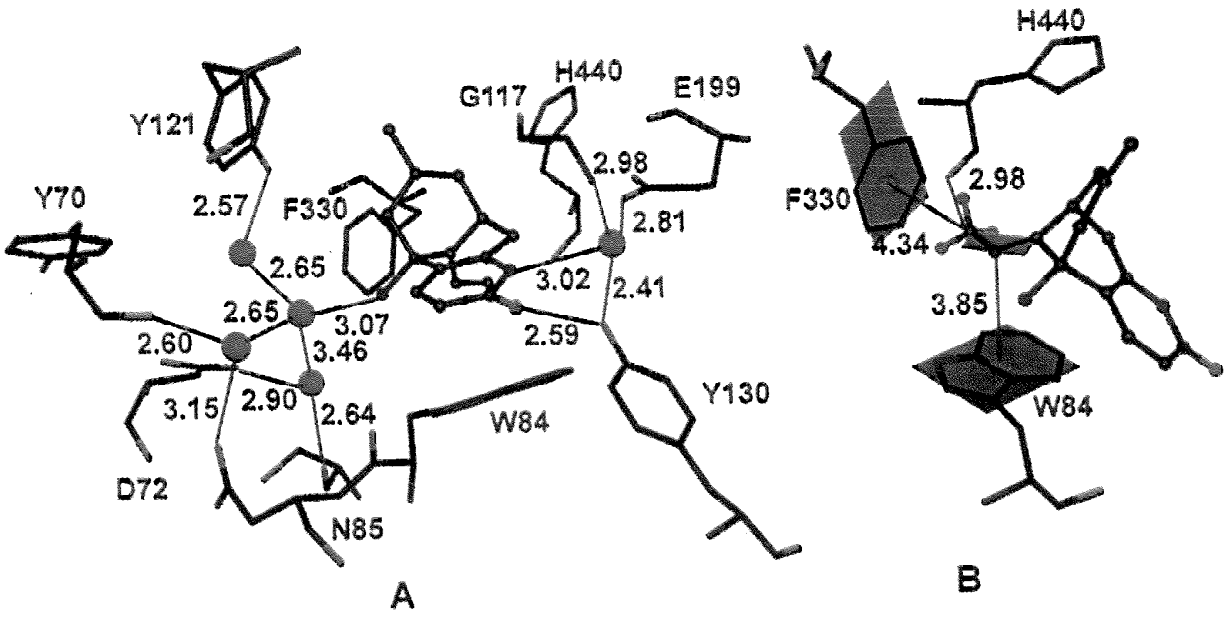

Fig. (1). The interactions of (–)-HupA with the active site of *Tc*AChE. (A) The hydrogen bonding net works. The water molecules are represented by red balls. (B) The C–H···π hydrogen bonds. All the distances are given in Å.

Kozikowski *et al.* [102, 103]. Pang *et al.* [104] in a docking study using the automated docking program, SYSDOC, suggested three possible orientations of HupA binding with AChE. One of the three candidate orientations differs only slightly from that of the crystal structure. Binding of HupA to the peripheral site, near Trp279, was also predicted. Although no evidence of that was found in the crystal structure, this docking result gave birth to design dual site binding (bivalent) HupA analogous inhibitors [66,67].

The crystal structure of HupA–*Tc*AChE complex took off the veil of HupA–AChE binding. It is surprising that HupA with such a strong affinity for AChE binds by means of so few direct contacts (Fig. 1). Only one strong hydrogen bond is formed between the pyridine oxygen of HupA and Tyr130. The ring nitrogen hydrogen binds to the protein through a water molecule. The hydrogen-bonding network is formed between the $-NH_3^+$ group and the protein through several waters (Fig. 1A). Unlike the expectation from intuition, the cationic group, $-NH_3^+$, does not form cation-π interactions with the nearest aromatic rings of Trp84 or Phe330 (Fig. 1B). However, the perfected orientation of HupA within the active site makes the ethylidene methyl group form cation-π-like (or termed C–H$\cdots\pi$ hydrogen bond) interaction with Phe330 (Fig. 1B). Quantum chemical calculation by means of MP2/6-31G* (unpublished data) indicated that this interaction contributes to the binding by ca. 1.3 kcal/mol. In addition, this methyl group forms a weak hydrogen bond with His440, its strength was estimated to be ca. 2.4 kcal/mol by using MP2/6-31 method (unpublished data). Based on the crystal structure, Raves *et al.* [97] unpuzzled the structure-activity relationship for a series of HupA analogs.

Recently, Dvir *et al.* [105] determined the crystal structures of the complexes of (–)-HupB, another natural analog of HupA extracted from the same herb *Huperzia serrata*, and (+)-HupA, a synthetic enantiomer of (–)-HupA with *Tc*AChE. The binding site of (–)-HupB within AChE is similar to that seen in the (–)-HupA–*Tc*AChE complex. All of the protein residues in the vicinity of the bound (–)-HupB, except for Phe330, are in the conformations very similar to those seen in the *Tc*AChE–(–)-HupA structure. Phe330 was refined in two alternative conformations in the *Tc*AChE–(–)-HupB structure, one (65% occupancy) very similar to that seen in the *Tc*AChE–(–)-HupA structure and another distinct conformation (35% occupancy). This is the first reported case of discrete disorder for Phe330 in a particular AChE structure. The water network around (–)-HupB is similar to that seen around (–)-HupA.

The binding site for (+)-HupA in *Tc*AChE also shares part of that for (–)-HupA. However, unlike its α-pyridone moiety which overlaps well with that of (–)-HupA, the ethylidene-methyl group of (+)-HupA points in the opposite direction to that of (–)-HupA, occupying similar space to that occupied by the three-carbon bridge of (–)-HupA in its *Tc*AChE complex. The bridghead carbon, to which the primary amine of (+)-HupA is attached, overlaps well with the corresponding carbon of (–)-HupA. However, because of

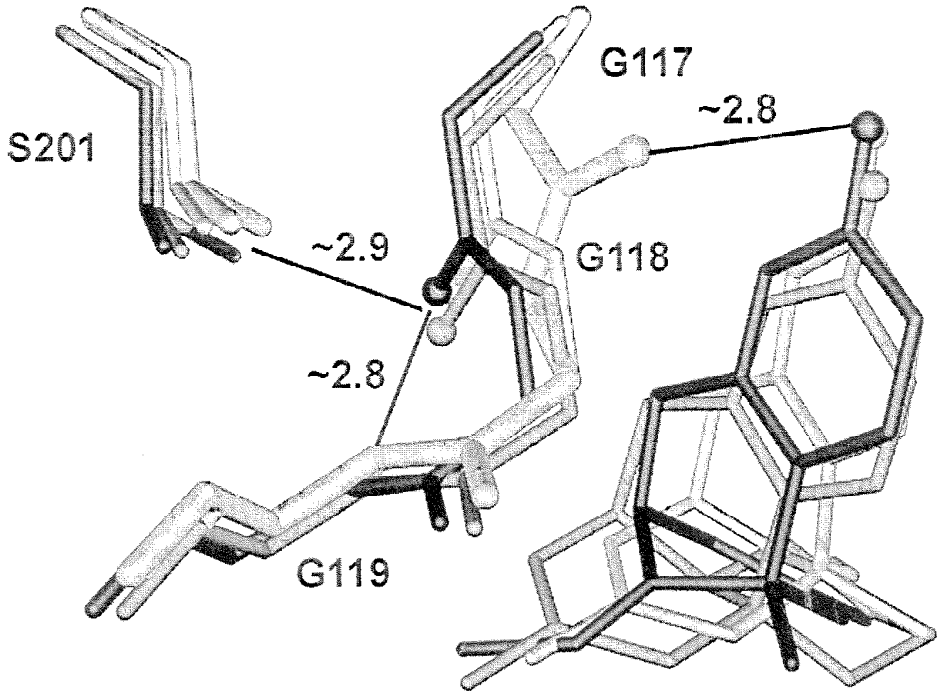

Fig. (2). Structural alignment (+)-HupA (black), (–)-HupA (grey) and HupB (hazel), and the flip of the peptide bond between Gly117 and Gly118 in the active site of *Tc*AChE upon binding of huperzine inhibitors. Four structures of *Tc*AChE are superimposed: native (thick grey; PDB code 2ACE) and three structures in complex with (+)-HupA (black), (–)-HupA (grey) and HupB (hazel). The distances are given in Å. The balls represent the carbonyl oxygen atoms of Gly117 and inhibitors.

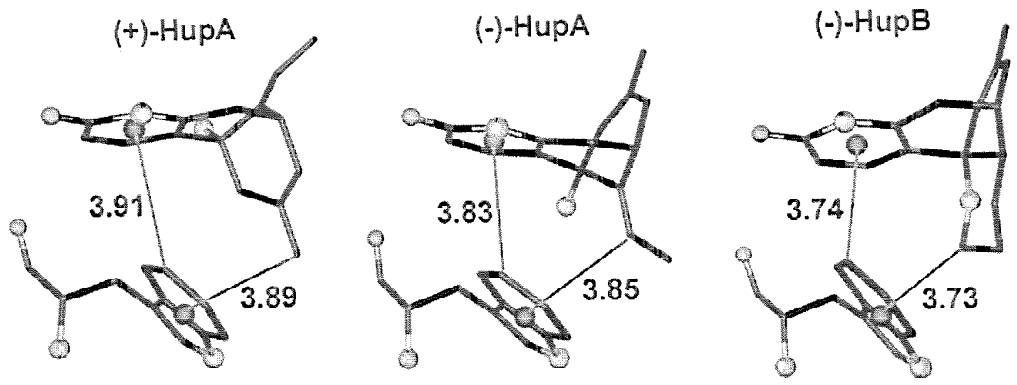

Fig. (3). The C H···π hydrogen bonds between HupA analogs and Trp84 of AChE. Hydrogen acceptors are represented by black balls. Distances from centroids of the aromatic rings (shown as black balls) to carbons of the corresponding C-H groups are given in Å. Large grey balls and small hazel balls respectively represent nitrogen and oxygen atoms.

opposite handedness, their amine atoms diverge, giving rise to different arrangements for the water networks that are in contact with these amines. The amino-acid residues of the binding sites for these two ligands are in very similar conformations (Fig. 2).

Comparing the structures of the three huperzines complexing with AChE, the common motif for the huperzines was addressed. Structurally, the α-pyridone moiety is common to all three inhibitors. For the three inhibitors, α-pyridone aligns well with each other within the active site of AChE, forming C–H···π hydrogen bonds with Trp84, in which the aromatic π-electrons of α-pyridone serve as the hydrogen acceptor for a C-H group in the indole ring of Trp84, while the aromatic π-electrons of the indole ring of Trp84 also serve as the hydrogen acceptor for a non-aromatic C H group in the ligands (Fig. 3). The mutual C–H···π hydrogen bonds may play a significant role in the recognition of the inhibitors with the protein, since Trp84 functions as a clamp to fix two different units of the inhibitors.

The other new finding of this study is that the "oxyanion" hole of AChE composed by Gly117, Gly118 and Gly119 are disrupted by the HupA analogous inhibitors. The carbonyl oxygens of all three HupA analogs appear to repel the carbonyl oxygen of Gly117, thus causing the peptide bond between Gly117 and Gly118 undergoing a peptide flip (Fig. 2). As a consequence, the position of the main chain nitrogen of Gly118 in the "oxyanion" hole of the native enzyme becomes occupied by the carbonyl of Gly117. Furthermore, the flipped conformation is stabilized by the hydrogen bonding of Gly117 to Gly119N and Ala201N, and the other two functional elements of the three-pronged oxyanion hole characteristic of cholinesterases. Therefore, these three HupA analogs have dual functions in inhibiting AChE catalytic activity: (1) occupy the active site of AChE so that the neurotransmitter ACh cannot access the active site; and (2) damage the oxyanion hole so that it cannot stabilize the structures of the transition states in the catalytic pathway. Additionally, kinetic determinations of these three inhibitors to *Tc*AChE were also performed in this study, and the dissociation constants of (+)-HupA, ( )-HupA and HupB were reported with the values of 4.30, 0.18 and 0.33 μM, respectively.

The crystal structure of huprine X **86** complexing with *Tc*AChE was also determined by Dvir *et al.* [98] at 2.1 Å resolution. Fig. 4 shows the interaction model of huprine X with *Tc*AChE and the comparison to that of tacrine and (-)-HupA. In general, huprine X binds to the anionic site and also hinders access to the esteratic site. Its aromatic portion occupies the same binding site as tacrine, stacking between the aromatic rings of Trp84 and Phe330, whereas the carbobicyclic unit occupies the same binding pocket as (-)-HupA. Its chlorine substituent was found to lie in a hydrophobic pocket interacting with the rings of the aromatic residues Trp432 and Phe330 and with the methyl groups of Met436 and Ile439.

The crystal structure is in agreement with the steady-state inhibition data showing that huprine X binds to hAChE and *Tc*AChE 28- and 54-fold, respectively, more tightly than tacrine. This difference stems from the fact that the aminoquinoline moiety of huprine X makes interactions similar to those made by tacrine, but additional bonds to the enzyme are formed by the huperzine-like substructure and the chlorine atom. Both tacrine and huprine X bind more tightly to *Tc*AChE than to hAChE, suggesting that their quinoline substructures interact better with Phe330 than with Tyr337 (the corresponding residue in the hAChE structure).

It was suggested that the flipped conformation of the Gly117 peptide bond, observed in the structures of the complexes between HupA analogs and *Tc*AChE (Fig. 2), might be necessary for the binding of HupA analogs to AChE [97,105]. This crystal structure oversets the early speculation that the flipping process might be relatively slow, and thus serves as the rate-limiting step in the association of HupA analogs with AChE. Because, similar to (–)-HupA, the k_{on} for huprine X to AChE is also low [98], the conformational flip at Gly117, was not observed in the huprine X–*Tc*AChE complex. Thus, the slow association rate of huprine X and HupA analogs may be attributed to the slow diffusion of its bulky rigid structure down to the active-site gorge.

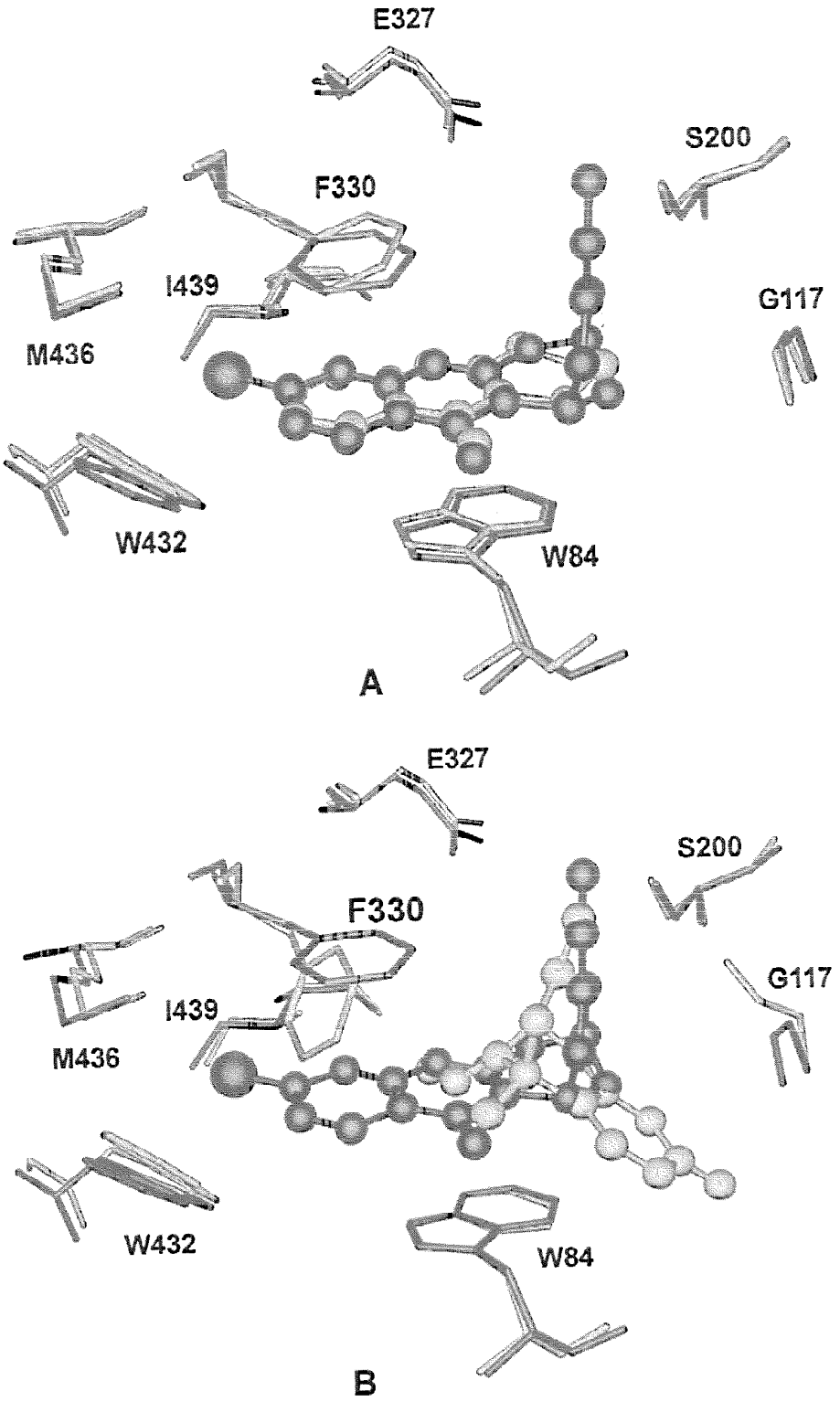

Fig. (4). Interaction model between huprine X and *Tc*AChE and comparison to tacrine (A) and (–)-HupA (B). The ligands are represented as ball-and-stick, and the main residues as stick model. Huprine X–AChE complex is colored in black and tacrine– and (–)-HupA–AChE complexes are colored in grey.

Wong *et al.* [100] determined the crystal structures of two bis-hupyridones, (*S,S*)-**30f** and (*S,S*)-**30h** (Table 2), the potent dual site inhibitors of AChE [67]. The structures revealed that one hupyridone unit bound to the "anionic" subsite of the active-site, as observed for the *Tc*AChE–(-)-HupA complex, and the second hupyridone unit was located near Trp279 in the "peripheral" anionic site at the top of the gorge. Both (*S,S*)-**30f** and (*S,S*)-**30h** fit the active-site gorge. The results confirm that the increased affinity of the dimeric HupA analogs for AChE is conferred by binding to the two "anionic" sites of the enzyme (Fig. 5). The structures gave a good explanation for the inhibition data showing that (*S,S*)-**30f** binds to *Tc*AChE ca. 6-7- and >170-fold more tightly than (*S,S*)-**30h** and (–)-HupA, respectively. In comparison with the crystal structure of mouse AChE, Wong *et al.* [100] rationalized the lower binding affinity of (*S,S*)-**30f** and (*S,S*)-**30h** for rat AChE, showing that (*S,S*)-**30h** binds ca. 3- and ca. 2-fold more tightly than (*S,S*)-**30f** and (–)-HupA, respectively.

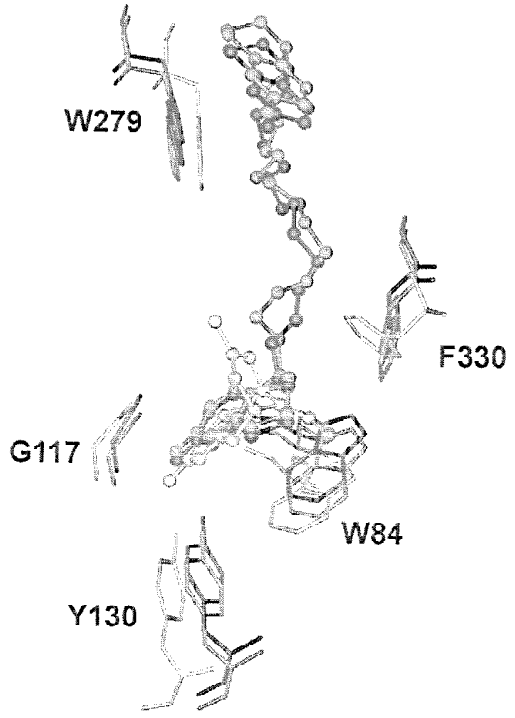

Fig. (5). Structural alignments of (*S,S*)-**30f** (black) and (*S,S*)-**30h** (hazel) with (–)-HupA (grey) in the active site of *Tc*AChE. The ligands are represented by ball-and-stick models.

7.3. Molecular Modeling and Simulations on HupA Analogs Binding with AChE

Before the structure of HupA–*Tc*AChE complex was available, modeling on the interaction between HupA and AChE by means of computational methods had been carried out. However, most of the modeling results did not give the correct binding orientation for HupA to AChE [101-104]. Only after the structure of HupA–*Tc*AChE complex was released; the researchers have a good starting point for modeling or simulating the binding of HupA analogs with AChE. In this section, we summarize some of the recent modeling and simulation results.

Based on the crystal structure of (–)-HupA–*Tc*AChE complex [97], Barril *et al.* [106] performed a molecular dynamics (MD) simulation on huprine **69** binding with AChE. Two different orientations of **69** in the binding pocket were tested in the MD simulation. Analysis of structural fluctuations, and the pattern of interactions between the inhibitor and enzyme favors one binding mode for the huprine, which adopts effectively some of the binding features of tacrine and (–)-HupA. The binding mode was recently verified by the X-ray crystal structure of huprine X–*Tc*AChE complex [98]. Based on the binding mode, the differences in inhibitory activity for a series of huprine derivatives were successfully predicted by using the free energy perturbation (FEP) approach. In addition, the effect of replacing Phe300 in the *Tc*AChE by Tyr, which is present in the hAChE was also investigated. The results indicated that the Phe330Tyr mutation is expected to have little effect on the binding affinities.

To explain the structure-activity relationships at a more quantitative level, Camps *et al.* [88] performed a molecular modeling study on a series of huprines using the same approach of Barril *et al.* [106]. The predicted free energy values are in general agreement with the inhibitory activity data of these inhibitors, and the modeling results rationalized the binding modes of these compounds to AChE.

Despite the progress in experimental and molecular simulation studies on AChE and its complexes [107], several questions are still open for the ligand–AChE binding. How do the inhibitors or substrates enter and leave the active-site gorge of AChE? What causes the peptide bond between Gly117 and Gly118 to be flipped by 180° in the HupA–*Tc*AChE complex compared with the native structure of AChE and other inhibitor complexes? What role the buried water molecules play for HupA binding and unbinding? To address these questions, we have investigated the entrance and leaving processes of HupA binding with the long active-site gorge of *Tc*AChE by using the steered molecular dynamics (SMD) [108] simulations [109]. The force required along the pathway and the total energy indicate that it is easier for HupA to bind to the active site of AChE than to disassociate from it, which interprets the previous experimental results about the long time residence of HupA at the atomic level for the first time. The direct hydrogen bonds, water bridges, and hydrophobic interactions were analyzed during two SMD simulations. Breaking the direct hydrogen bond contributes a lot of pulling force. The steric hindrance of bottleneck might be the most important factor producing the maximal rupture force for HupA leaving the binding site. However, the bottleneck has a little effect on binding process of HupA with AChE. Asp72 forms a lot of water bridges throughout HupA leaving and entering the AChE binding gorge, acting as a clamp to take out HupA from or put HupA into the active site. The flip of the peptide bond between Gly117 and Gly118 has been detected by the normal MD and SMD simulations. The simulation results indicate that this flip phenomenon may be an intrinsic property of AChE, and the Gly117–Gly118 peptide bond in

both HupA bound and unbound AChE structures tends to adopt a native enzyme structure. Without water molecules the rupture force for HupA to leave the binding gorge is increased up to 1500 pN, while for the similar process in

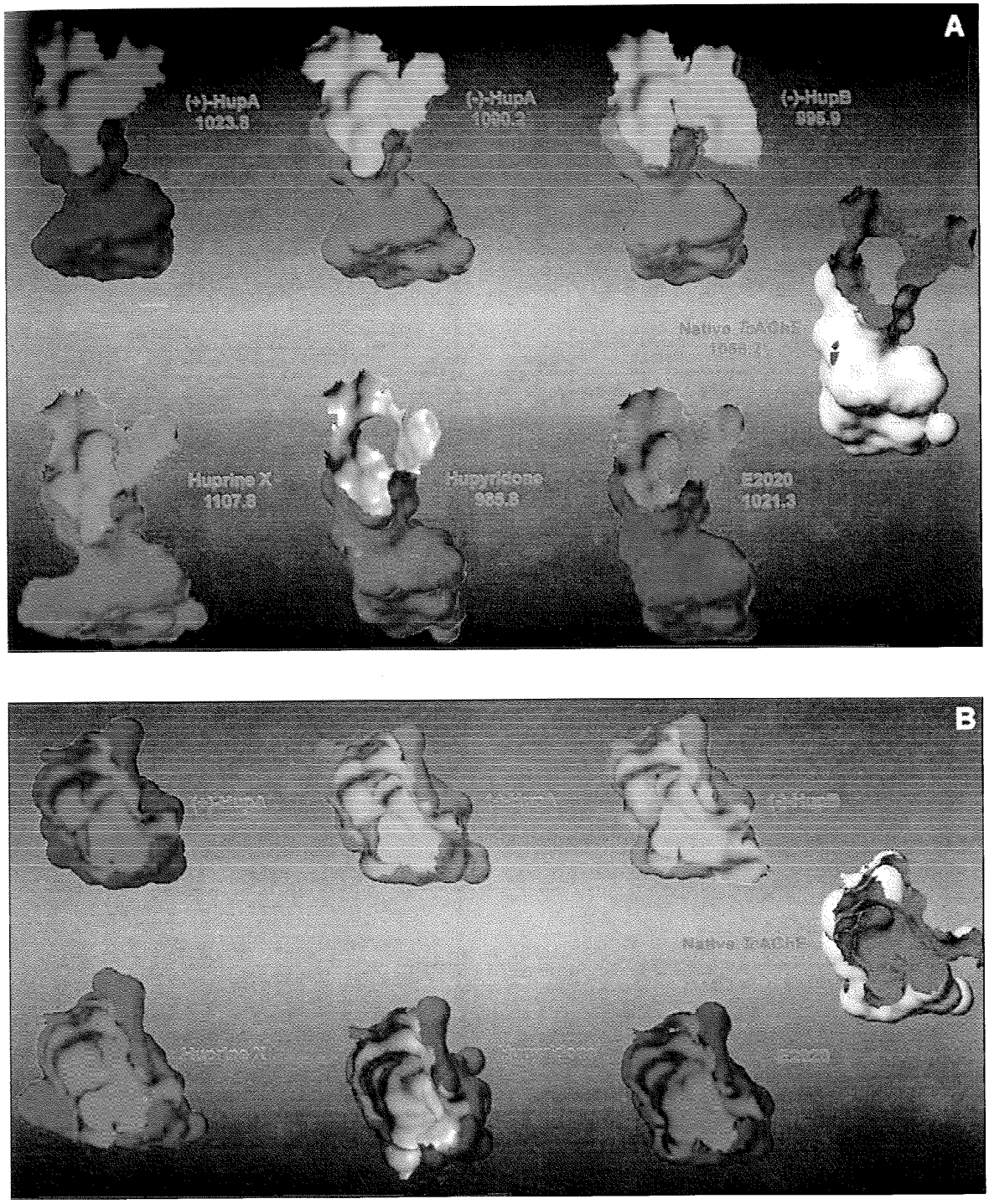

Fig. (6). The surface expressions of the binding gorge pockets of *Tc*AChE and its complexes with (+)-HupA, (–)-HupA, (–)-HupB, huprine X, hupyridone and E2020. (A) Side-view of the binding pockets. (B) Top-view of the binding pockets. The values in (A) are the volumes of the binding gorges given in $Å^3$.

aqueous solution the greatest force is about 800 pN. It means that water molecules in the binding gorge act as lubricant to facilitate HupA entering or leaving the binding gorge.

Recently, we made a comparison for the binding gorges of AChE and its complexes with HupA analogs, *viz.* (+)-HupA, (–)-HupA, (–)-HupB, huprine X, hupyridone and E2020 [unpublished data]. The surface expressions of the gorges of these inhibitor–*Tc*AChE complexes are shown in Fig. 6. Comparing with the native structure of *Tc*AChE, the binding gorges of the complexes are in general reduced except for huprine X (Fig. 6A). Huprine X is a hybride of (-)-HupA and tacrine, which is the most "fat" compound among these HupA analogs. Therefore, binding of huprine X with AChE, inflates the binding gorge. Another phenomenon is found from this modeling that the bottleneck of the binding gorge, comprising mainly Tyr121 and Phe330, is open in the native and dual site inhibitor (hupyridone and E2020) complexes; while in the active site inhibitor complexes, the bottleneck is closed (Fig. 6B).

CONCLUSIONS

During the past four years, the great interest in HupA has been essentially inspired by two facts. First, HupA has better penetration through blood-brain barrier, higher oral bioavailability, and longer duration of AChE inhibitory action in comparison with other well-known AChEIs, such as physostigmine, galanthamine, tacrine and donepezil. HupA exhibited the memory-enhancing efficacy in a variety of animal models of cognitive impairment. Clinical trials have demonstrated that HupA produced significant improvements in memory deficiencies in aged and AD patients. The HupA–AChE complex has a longer life than other prophylactic sequestering agents, so HupA has now been proposed as a pretreatment drug for organophosphonates nerve agents. Second, recent studies have proved that HupA possesses different pharmacological actions other than hydrolysis of synaptic ACh. These non-cholinergic roles, for instance, the antagonist effect on NMDA receptor, the protection of neuronal cells against Aβ, free radicals and hypoxia-ischemia induced injury, could be important too in AD treatment. The therapeutic effects of HupA are probably based on a multi-target mechanism.

X-ray crystallography and molecular modeling studies of HupA analog–AChE interactions are valuable for the rational design of new analogs with improved therapeutic profiles. Several potent AChEIs, such as huprines and hupyridones, were designed based on such kinds of studies. Recently, the crystal structures of the *Tc*AChE complexes of these new HupA analogs have been determined, revealing the interactions between AChE and inhibitors at the atomic level. This is beneficial to designing new analogs in future.

ACKNOWLEDGEMENTS

We thank Prof. Wei-Min Dai for his encouragement in writing this review and for many useful suggestions. We gratefully acknowledge financial support from National Natural Science Foundation of China (Grants 29725203, 20102007, 29725203, 20072042, 39170529, 39170860, 39770846 and 30070865), the State Key Program of Basic Research of China (Grant 2002CB512802), and the 863 Hi-Tech Program of China (Grants 2002AA233061, 2001AA235051 and 2001AA235041).

ABBREVIATIONS

Aβ	=	β-Amyloid peptide
ACh	=	Acetylcholine
AChE	=	Acetylcholinesterase
hAChE	=	Human acetylcholinesterase
*Tc*AChE	=	*Torpedo californica* acetylcholinesterase
AChEI	=	Acetylcholinesterase inhibitor
AD	=	Alzheimer's disease
AIBN	=	Azobisisobutyronitrile
BChE	=	Butyrylcholinesterase
CAT	=	Catalase
GABA	=	γ-amino-*n*-butyric acid
GSH-Px	=	Glutathione peroxidase
HupA	=	(–)-Huperzine A
HupB	=	(–)-Huperzine B
MD	=	Molecular Dynamics
MDA	=	Malondialdehyde
MK-801	=	Dizocilpine
NMDA	=	*N*-Methyl-*D*-aspartate
OGD	=	Oxygen-glucose deprivation
PC12	=	Pheochromocytoma line PC12
ROS	=	Reactive oxygen species
SOD	=	Superoxide dismutase
TMG	=	Tetramethylguanidine

REFERENCES

[1] Launer, L.J.; Fratiglioni, L.; Andersen, K.; Breteler, M.M.B.; Copeland, R.J.M.; Dartigues, J.-F.; Lobo, A.; Martinez-Lage, J.; Soininen, H.; Hofman, A. In *Alzheimer's Disease and Related Disorder: Etiology, Pathogenesis and Therapeutics*; Iqbal, K.; Swaab, D.F.; Winblad, B.; Wisniewski, H.M. Eds., John Wiley & Sons, New York, **1999**, p.9.

[2] Schenk, D.; Barbour, R.; Dunn, W.; Gordon, G.; Grajeda, H.; Guido, T.; Hu, K., Huang, J.; Johnson-Wood, K.; Khan, K.; Kholodenko, D.; Lee, M.; Liao, Z.; Lieberburg, I.; Motter, R.; Mutter, L.; Soriano, F.; Shopp, G.; Vasquez, N.; Vandevert, C.; Walker, S.; Wogulis, M.; Yednock, T.; Games, D.; Seubert, P. *Nature*, **1999**, *400*, 173.

[3] Gualtieri, F.; Deu, S.; Manetti, D.; Romanelli, M. N. *Farmacologie*, **1995**, *50*, 489.

[4] Bartus, R. T.; Dean, R. L.; Beer, B.; Lippa, A. S. *Science*, **1982**, *217*, 408.

[5] Sugimoto, H.; Yamanishi, Y.; Iimura, Y.; Kawakami, Y. *Curr. Med. Chem.*, **2000**, 7, 303.

[6] Alvarez, A.; Alarcon, R.; Opazo, C.; Campos, E.O.; Munoz, F.J.; Calderon, F.H.; Dajas, F.; Gentry, M.K.; Doctor, B.P.; DeMello, F.G.; Inestrosa, N.C. *J. Neurosci.*, **1998**, *18*, 3213.

[7] Kozikowski, A.P.; Tückmantel, W. *Acc. Chem. Res.*, **1999**, *32*, 641.

[8] Tang, X.C.; He, X.C.; Bai, D.L. *Drugs Future*, **1999**, *24*, 647.
[9] Bai, D.L.; Tang, X.C.; He, X.C. *Curr. Med. Chem.*, **2000**, *7*, 355.
[10] Zeng, F.X.; Jiang, H.L.; Yang, Y.S.; Chen, K.X.; Ji, R.Y. *Progress in Chemistry*, **2000**, *12*, 63.
[11] Tang, X.C.; Han, Y.F. *CNS Drug Rev.*, **1999**, *5*, 281.
[12] Sun, Q.Q.; Xu, S.S.; Pan, J.L.; Guo, H.M.; Cao, W.Q. *Acta Parmacol. Sin.*, **1999**, *20*, 601.
[13] Xu, S.S.; Cai, Z.Y.; Qu, Z.W.; Yang, R.M.; Cai, Y.L.; Wang, G.Q.; Su, X.Q.; Zhong, X.S.; Cheng, R.Y.; Xu, W.A.; Li, J.X.; Feng, B. *Acta Parmacol. Sin.*, **1999**, *20*, 486.
[14] Ma, Y.X.; Zhu, Y.; Gu, Y.D. Yu, Z.Y.; Yu, S.M.; Ye, Y.Z. *Ann. NY. Acad. Sci.*, **1998**, *854*, 506.
[15] Ma, Y.X.; Zhu, Y.; Gu, Y.D.; Yu, Z.Y.; Yu, S.M.; Ye, Y.Z. *N-S Arch Pharmacol.*, **1998**, *358*, Suppl. 1, P35194.
[16] Ashani, Y.; Grunwald, J.; Alkalai, D.; Cohen, G.; Raveh, L. *Med. Def. Biosci. Rev., Proc.*, **1996**, *1*, 105.
[17] Lallement, G.; Veyret, J., Masqueliez, C.; Aubriot, S.; Burckhart, M. F.; Baubichon, D. *Fundam. Clin. Pharmacol.*, **1997**, *11*, 387.
[18] Lallement, G. *Ann. Pharm. Fr.*, **2000**, *58*, 13.
[19] Tonduli, L.S.; Testylier, G.; Masqueliez, C.; Lallement, G.; Monmaur, P. *Neurotoxicology*, **2001**, *22*, 29.
[20] Lallement, G.; Foquin, A.; Dorandeu, F.; Baubichon, D.; Aubriot, S.; Carpentier, P. *Drug Chem. Toxicol.*, **2001**, *24*, 151.
[21] Lallement, G.; Foquin, A.; Dorandeu, F. Baubichon, D.; Carpentier, P. *Drug Chem. Toxicol.*, **2001**, *24*, 165.
[22] Lallement, G., Demoncheaux, J-P.; Foquin, A.; Baubichon, D.; Galonnier, M.; Clarencon, D.; Dorandeu, F. *Drug Chem. Toxicol.*, (1997) **2002**, *25*, 309.
[23] Ainge, G.D.; Lorimer, S.D.; Gerard, P.J.; Ruf, L.D. *J. Agricul. Food Chem.*, **2002**, *50*, 491.
[24] Xiong, Z.Q.; Cheng, D.H.; Tang, X.C. *Acta Pharmacol. Sin.*, **1998**, *19*, 128.
[25] Ye, J.W.; Shang, Y.Z.; Wang, Z.M.; Tang, X.C. *Acta Pharmacol. Sin.*, **2000**, *21*, 65.
[26] Gao, Y.; Tang, X.C.; Guan, L.C.; Kuang, P.Z. *Acta Pharmacol. Sin.*, **2000**, *21*, 1169.
[27] Ou, L.Y.; Tang, X.C.; Cai, J.X. *Eur. J. Pharmacol.*, **2001**, *433*, 151.
[28] Filliat, P.; Foquin, A.; Lallement, G. *Drug Chem. Toxicol.*, (1977) **2002**, *25*, 9.
[29] Schmidt, B.H.; Van Der Staay, F.J. *Int. J. Geriatr. Psychopharmacol.*, **1998**, *1*, 134.
[30] Ved, H.S.; Koenig, M.L.; Dave, J.R.; Doctor, B.P. *NeuroReport*, **1997**, *8*, 963.
[31] Wang, X.-D,; Chen, X.-Q.; Yang, H.-H.; Hu, G.-Y. *Neurosci. Lett.*, **1999**, *272*, 21
[32] Zhang, Y.-H.; Chen, X.-Q.; Yang, H.-H.; Jin, G.-Y.; Bai, D.-L.; Hu, G.-Y. *Neurosci. Lett.*, **2000**, *295*, 116
[33] Zhang, J.-M.; Hu, G.-Y. *Neuroscience*, **2001**, *105*, 663.
[34] Zhang, Y.H.; Zhao, X.Y.; Chen, X.Q.; Wang, Y.; Yang, H.H.; Hu, G.-Y. *Neurosci. Lett.*, **2002**, *319*, 107.
[35] Gordon, R.K., Nigam, S.V., Weitz, J.A.; Dave, J.R.; Doctor, B.P.; Ved, H.S. *J. Appl. Toxicol.*, **2001**, *21(suppl. 1)*, S47.
[36] Xiao, X.Q.; Wang, R.; Tang, X.C. *J. Neurosci. Res.*, **2000**, *61*, 564.
[37] Xiao, X.Q.; Wang, R.; Han, Y.F.; Tang, X.C. *Neurosci. Lett.*, **2000**, *286*, 155.
[38] Ye, L.; Qiao, J.T. *Neurosci. Lett.*, **1999**, *275*, 187.
[39] Wang, R.; Zhang, H.Y.; Tang, X.C. *Eur. J. Pharmacol.*, **2001**, *421*, 149.
[40] Ved, H.; Dave, J.; Garcia, G.; Doctor, B. *FASER J.*, **2001**, *15*, pt.2, A1160.
[41] Xiao, X.Q.; Zhang, H.Y.; Tang, X.C. J. *Neurosci. Res.*, **2002**, *67*, 30.
[42] Zhang, H.Y.; Liang Y.Q.; Tang, X.C.; He, X.C.; Bai, D.L. *Neurosci. Lett.*, **2002**, *317*, 143.
[43] Shang, Y.Z.; Ye, J.W.; Tang, X.C. *Acta Pharmacol. Sin.*, **1999**, *20*, 824.
[44] Xiao, X.Q.; Yang, J.W.; Tang, X.C. *Neurosci. Lett.*, **1999**, *275*, 73.
[45] Wang, L.M.; Han, Y.F.; Tang, X.C. *Eur. J. Pharmacol.*, **2000**, *398*, 65.
[46] Zhou, J.; Zhang, H.Y.; Tang, X.C. *Neurosci. Lett.*, **2001**, *313*, 137.
[47] Wang, L.S.; Zhou, J.; Shao, X.M.; Tang, X.C. *Brain Res.*, **2002**, *949*, 162.
[48] Zhou, J.; Tang, X.C. *FEBS Lett.*, **2002**, *526*, 21.
[49] Zhou, J.; Fu, Y.; Tang, X.C. *Neurosci. Lett.*, **2001**, *306*, 53.
[50] Zhou, J.; Fu, Y.; Tang, X.C. *Neuroreport*, **2001**, *12*, 2073.
[51] Wang, R.; Xiao, X.Q.; Tang, X.C. *Neuroreport*, **2001**, *12*, 2629.
[52] Zhao, H.W.; Li, X.Y. *Acta Pharmacol. Sin.*, **1999**, *20*, 941.
[53] Li, Y.; Hu G.Y.; *Neurosci. Lett.*, **2002**, *324*, 25.
[54] Li, Y.; Hu G.Y.; *Neurosci. Lett.*, **2002**, *329*, 153.
[55] Galeotti, N.; Ghelardini, C.; Di Cesare Mannelli, L.; Bartolini, A. *Drug Develop. Res.*, **2001**, *54*, 19.
[56] Kozikowski, A.P.; Campiani, G.; Tückmantel, W. *Heterocycles*, **1994**, *39*, 101.
[57] Camps, P.; Contreras, J. *Synth. Commun.*, **1996**, *26*, 9.
[58] Kozikowski, A.P.; Reddy, E.R.; Miller, C.P. *J. Chem. Soc., Perkin Trans.*, **1990**, 195.
[59] Camps, P.; Contreras, J.; El Achab, R.; Morral, J.; Muñoz-Torrero, D.; Font-Bardia, M.; Solans, X.; Badia, A.; Vivas, N.M. *Tetrahedron*, **2000**, *56*, 4541.
[60] Chassaing, C.; Haudrechy, A.; Langlois, Y. *Tetrahedron Lett.*, **1999**, *40*, 8805.
[61] Haudrechy, A.; Chassaing, C.; Riche, C.; Langlois, Y. *Tetrahedron*, **2000**, *56*, 3181.
[62] Keneko, S.; Yashino, T.; Katoh, T.; Terashima, S. *Tetrahedron: Asymmetry*, **1997**, *8*, 829.
[63] He, X.C.; Wang, B.; Bai, D.L. *Tetrahedron Lett.* **1998**, *39*, 411.
[64] He, X.C.; Wang, B.; Yu, G.L.; Bai, D.L. *Tetrahedron: Asymmetry*, **2001**, *12*, 3213.
[65] Lee, I.Y.C.; Jung, M.H.; Lee, H.W.; Yang, J.Y. *Tetrahedron Lett.*, **2002**, *43*, 2407.
[66] Carlier, P.R.; Du, D.M.; Han, Y.F.; Liu, J.; Pang, Y.P. *Bioorg. Med. Chem. Lett.*, **1999**, *9*, 2335.
[67] Carlier, P.R.; Du, D.M.; Han, Y.F.; Liu, J.; Perola, E.; Williams, I.D.; Pang, Y.P. *Angew. Chem., Int. Ed.*, **2000**, *39*, 1775.
[68] Camps, P.; Munoz-Torrero, D. *Mini-Rev. Med. Chem.*, **2001**, *1*, 163.
[69] Jin, G.Y.; He, X.Ch.; Zhang, H.Y.; Bai, D.L. *Chin. Chem. Lett.*, **2002**, *13*, 23.
[70] Jin, G.Y.; Luo, X.M.; He, X.C.; Jiang, H.L.; Zhang, H.Y.; Bai. D.L. *Drug Res.*, **2003**, *53, in Pess.*
[71] Zeng, F.X.; Jiang, H.L.; Zhai, Y.F.; Liu, D.X.; Zhang, H.Y.; Chen, K.X.; Ji, R.Y. *Acta Chim. Sin.*, **2000**, *58*, 580.
[72] Zeng, F.X.; Jiang, H.L.; Zhai, Y.F.; Zhang, H.Y.; Chen, K.X.; Ji, R.Y. *Bioorg. Med. Chem. Lett.*, **1999**, *9*, 3279.
[73] Zhou, G.-C.; Zhu, D.-Y. *Bioorg. Med. Chem. Lett.*, **2000**, *10*, 2055.
[74] Camps, P.; Contreras, J.; Morral, J.; Munoz-Torrero, D.; Font-Bardia, M.; Slans, X. *Tetrahedron*, **1999**, *55*, 8481.
[75] Camps, P.; Munoz-Torrero, D.; Simon, M. *Synth. Commun.*, **2001**, *31*, 3507.
[76] Foricher, Y.; Mann, J. *Tetrahedron Lett.*, **2000**, *41*, 2007.
[77] Kozikowski, A.P.; Ding, Q.; Saxena, A.; Doctor, B.P. *Bioorg. Med. Chem. Lett.*, **1996**, *6*, 259.
[78] Rajendran, V.; Prakash, K. R. C.; Ved, H.S.; Saxena, A.; Doctor, B.P.; Kozikowski, A.P. *Bioorg. Med. Chem. Lett.*, **2000**, *10*, 2467.
[79] Khiari, J.; Hassine, B.B.; Gravel, D. Comptes Rendus de l'Academie des Sciences, Serie IIc: Chimie, **2001**, 4, 705.
[80] Wang, B.; He, X.C.; Bai, D.L. *Acta Pharm. Sin.*, **1999**, *34*, 434.
[81] Hogenauer, K.; Baumann, K.; Mulzer, J. *Tetrahedron Lett.*, **2000**, *41*, 9229.
[82] Hogenauer, K.; Baumann, K.; Enz, A.; Mulzer, J. *Bioorg. Med. Chem. Lett.*, **2001**, *11*, 2627.
[83] Rajendran, V.; Rong, S.-B.; Saxena, A.; Doctor, B.P.; Kozikowski, A.P. *Tetrahedron Lett.*, **2001**, *42*, 5359.
[84] Rajendran, V.; Saxena, A.; Doctor, B.P.; Kozikowski, A.P. *Bioorg. Med. Chem. Lett.*, **2002**, *12*, 1521.
[85] Badia, A.; Baños, J.E.; Camps, P.; Contreras, J.; Görbig, D.M.; Muñoz-Torrero, D.; Simon, M.; Vivas, N.M. *Bioorg. Med. Chem.*, **1998**, *6*, 427.
[86] Camps, P.; El Achab, R.; Görbig, D.M.; Morral, J.; Muñoz-Torrero, D.; Badia, A.; Baños, J.E.; Vivas, N.M.; Barril, X.; Orozco, M.; Luque, F.J. *J. Med. Chem.*, **1999**, *42*, 3227.
[87] Camps, P.; Cusack, B.; Mallender, W.D.; El Achab, R.; Morral, J.; Muñoz-Torrero, D.; Rosenberry, T.L. *Mol. Pharmacol.*, **2000**, *57*, 409.
[88] Camps, P.; El Achab, R.; Morral, J.; Muñoz-Torrero, D.; Badia, A.; Baños, J.E.; Vivas, N.M.; Barril, X.; Orozco, M.; Luque, F.J. *J. Med. Chem.*, **2000**, *43*, 4657.
[89] Camps, P.; Contreras, J.; Font-Bardia, M.; Morral, J.; Muñoz-Torrero, D.; Solans, X. *Tetrahedron: Asymmetry*, **1998**, *9*, 835.
[90] Camps, P.; Gomez, E. Muñoz-Torrero, D.; Arno, M. *Tetrahedron: Asymmetry*, **2001**, *12*, 2909.
[91] Ros, E.; Aleu, J.; deAranda, I.G.; Muñoz-Torrero, D.; Camps, P.; Badia, A.; Marsal, J.; Solsona, C. *Eur. J. Pharmacol.*, **2001**, *421*, 77.

[92] Camps, P.; Gomez, E.; Muñoz-Torrero, D.; Badia, A.; Vivas, N.M.; Barril, X.; Orozco, M.; Luque, F.J. *J. Med. Chem.*, **2001**, *44*, 4733.
[93] Sussman, J. L.; Harel, M.; Frolow, F.; Oefner, C.; Goldman, A.; Toker, L.; Silman, I. *Science*, **1991**, *253*, 872.
[94] Pang, Y.-P.; Quiram, P.; Jelacic, T.; Hong, F.; Brimijoin, S. *J. Biol. Chem.*, **1996**, *271*, 23646.
[95] Carlier, P.R., Han, Y.F., Chow, E. S.-H., Li, C. P.-L., Wang, H.; Lieu,T.X.; Wong, H.S.; Pang, Y.-P. *Bioorg. Med. Chem.*, **1999**, *7*, 351.
[96] Harel, M.; Schalk, I.; Ehret-Sabatier, L.; Bouet, F.; Goeldner, M.; Hirth, C.; Axelsen, P. H.; Silman, I.; Sussman, J. L. *Proc. Natl. Acad. Sci. USA*, **1993**, *90*, 9031.
[97] Raves, M. L.; Harel, M.; Pang, Y. P.; Silman, I.; Kozikowski, A. P.; Sussman, J. L. *Nat. Struct. Biol.*, **1997**, *4*, 57.
[98] Dvir, H.; Wong, D. M.; Harel, M.; Barril, X.; Orozco, M.; Luque, F.J.; Muñoz-Torrero, D.; Camps, P.; Rosenberry, T. L.; Silman, I.; Sussman, J.L. *Biochemistry*, **2002**, *41*, 2970.
[99] Felder, C. E.; Harel, M.; Silman, I.; Sussman, J. L. *Acta Crystallogr.*, **2002**, *D58*, 1765.
[100] Wong, D.M.; Greenblatt, H.M.; Dvir, H.; Carlier, P.R.; Han, Y.-F.; Pang, Y.P.; Silman, I.; Sussman, J.L. *J. Am. Chem. Soc.*, **2003**, *125*, 363.
[101] Kozikowski, A. P. *et al. J. Org. Chem.*, **1991**, *56*, 4636.
[102] Ashani, Y.; *Mol Pharmacol*, **1994**, *45*, 555.
[103] Saxena, A. *Prot. Sci.*, **1994**, *3*, 1770.
[104] Pang, Y.-P.; Kozikowski, A. P. J. *Computer-Aided Mol. Design*, **1994**, *8*, 669.
[105] H. Dvir, H., Jiang, H.L., Wong, D.M.; Harel, M.; Chetrit, M.; He, X.C.; Jin, G.Y.; Yu, G.L.; Tang, C.X.; Silman, I.; Bai, D.L.; Sussman, J. L., *Biochemistry*, **2002**, *41*, 10810.
[106] Barril, X.; Orozco, M.; Luque, F.J. *J. Med. Chem.*, **1999**, *42*, 5110.
[107] Shen, T.; Tai, K.; Henchman, R.H.; McCammon, J.A. *Acc. Chem. Res.*, **2002**, *35*, 321.
[108] Israelewitz, B.; Gao, M.; Schulten, K. *Curr. Opin. Struc. Biol.*, **2001**, *11*, 224.
[109] Xu, Y.; Shen, J.; Luo, X.; Silman, I.; Sussman, J. L.; Jiang, H.; Chen, K. *J. Am. Chem. Soc.*, to be published.